



TITLE:

Kinetic model for the phase transition of the van der Waals fluid

AUTHOR(S):

Takata, Shigeru; Matsumoto, Takuya; Hattori, Masanari

CITATION:

Takata, Shigeru ...[et al]. Kinetic model for the phase transition of the van der Waals fluid. *Physical Review E* 2021, 103(6): 062110.

ISSUE DATE:

2021-06




URL:

<http://hdl.handle.net/2433/269543>

RIGHT:

© 2021 American Physical Society

Kinetic model for the phase transition of the van der Waals fluid

 Shigeru Takata ^{1,2,*}, Takuya Matsumoto ¹ and Masanari Hattori ^{1,2}
¹*Department of Aeronautics and Astronautics, Graduate School of Engineering, Kyoto University, Kyoto 615–8540, Japan*
²*Research Project of Fluid Science and Engineering, Advanced Engineering Research Center, Kyoto University, Kyoto 615-8540, Japan*


(Received 11 March 2021; revised 10 May 2021; accepted 12 May 2021; published 3 June 2021)

This is a continuation of previous works [S. Takata and T. Noguchi, *J. Stat. Phys.* **172**, 880 (2018); S. Takata, T. Matsumoto, A. Hirahara, and M. Hattori, *Phys. Rev. E* **98**, 052123 (2018)]. The simple model proposed in the previous works is extended to be free from the isothermal assumption. The new model conserves the total mass, momentum, and energy in the periodic domain. A monotone functional is found, assuring the H theorem for the new model. Different approaches are taken to tell apart the stable, the metastable, and the unstable uniform equilibrium state. Numerical simulations are also conducted for spatially one-dimensional cases to demonstrate various features occurring in the time evolution process. A prediction method for the profile at the stationary state is discussed as well.

 DOI: [10.1103/PhysRevE.103.062110](https://doi.org/10.1103/PhysRevE.103.062110)

I. INTRODUCTION

A gas-liquid phase transition is a very familiar phenomenon found everywhere in our daily lives. The dryness of wet clothes, the whitening of exhaled breath in winter, and the formation of clouds in the sky are all involved in this phenomenon. In engineering applications, for example, moist air is avoided to use in a supersonic wind tunnel to prevent undesired condensation such as the generation of condensation shock waves. The physics of phase transitions thus pops up in many phenomena around us and in engineering applications. The conventional thermofluid dynamics is a powerful phenomenology that explains many of them, but it is still not sufficient to discern the phenomena in strong nonequilibrium processes that far exceed its application range.

To shed light on the nonequilibrium aspects of these phenomena, it is often required to incorporate more microscopic considerations. One such attempt is the molecular dynamics (MD) that treats the thermofluid as a particle system according to the laws of mechanics. In the present paper, we shall take another approach, namely, the kinetic theory that is in between the conventional macroscopic continuous approach and the MD.

In the kinetic theory, the molecular movement is not tracked one by one. Rather, the collective behavior of molecules is investigated through the velocity distribution function (VDF) of molecules [1–3]. Such an approach is by far less demanding in computational resources than the MD but still has the advantage over the macroscopic continuous approach in its wider applicability regardless of whether the target system is in equilibrium or not. The kinetic theory has been developing since its foundation by Boltzmann for rarefied gases based on two-body collision dynamics. Yet, his

celebrated equation, the Boltzmann equation, is by itself not enough to describe the gas-liquid two-phase system.

Attempts to extend Boltzmann's treatment to moderately dense gases date back to the celebrated work by Enskog [4]. Enskog proposed an extension of the Boltzmann equation, which is called the Enskog equation [4,5] today, by taking account of the finite-size effects of a molecule in the collision integral. In the Enskog equation, the molecules are treated as rigid spheres, and thus they interact each other only repulsively. Therefore, in application to the phase transition problem, the Enskog–Vlasov equation [6], which incorporates the effect of attractive interaction over a wider range than the repulsive force as a self-consistent Vlasov external force term, is often adopted in recent kinetic studies [7–12]. The kinetic approach has also been taken in a very recent attempt [13] to put a firm foundation on the fluid model of a gas-liquid interface. The kinetic studies on dense gases, targeting the understanding of phase transitions, have become more and more active recently.

The Enskog–Vlasov equation is a legitimate choice to observe the details of phenomena down to the molecular size scale, but in many cases such details are not necessarily required. Therefore, the authors proposed the presumably simplest kinetic model that is equipped with the essential mechanism required for the phase-transition descriptions under the isothermal assumption [14,15]. In the continuum limit, the model recovers a Cahn–Hilliard-type equation for the fluid density. The stability of the uniform equilibrium state in that limit was investigated in Ref. [14] by both linear stability analysis and numerical simulations. In Ref. [15], the transition process from the uniform equilibrium state to a new two-phase stationary state was investigated in detail, shedding light on the nonequilibrium aspects. In particular, it was numerically confirmed that there is a functional that changes monotonically in time, the manifestation of the H theorem in that model.

In the present paper, motivated by the success of the above simple model in exhibiting the intended performance, a new

*takata.shigeru.4a@kyoto-u.ac.jp

kinetic model that conserves not only the total mass but also the total momentum and energy in a system is proposed as an extension of the previous model. Consideration of the energy conservation implies that the isothermal assumption in the previous model is no longer made. Consequently, as will be seen later, the proposed model is able to handle the energy exchanges occurring in the formation of the two-phase interface quantitatively. Furthermore, it is still equipped with a functional that changes monotonically in time. Hence, the proposed model is more suitable than the original Enskog equation for the discussion of phase transitions, because the original Enskog equation does not satisfy the counterpart property exactly. This demerit of the Enskog equation was resolved in the modified Enskog equation [16–19]. However, there is still a gap to be overcome in using the modified equation for practical/numerical analyses. Here is the merit of proposing a kinetic model that conforms to the H theorem. Thus, the time evolution processes observed in numerical simulations will be reported in detail in the present paper, as well as the analyses of the stable, the metastable, and the unstable condition.

The paper is organized as follows. First, the new model is proposed in Sec. II. Then, the mass, the momentum, and the energy balance derived from the model are presented in Sec. III, where some factors occurring in the model are shown to play a role of recovering the conventional form of mass, momentum, and energy equations. Next, in Sec. IV, the proposed model is shown to have the property corresponding to Boltzmann's H theorem. The property is used to discuss the stability of the uniform equilibrium state in Sec. V. In Sec. VI, the dimensionless descriptions are introduced to clarify the parameters that characterize the problem, which is followed by the presentation of some numerical simulation results for a spatially one-dimensional system in Sec. VII A. In Sec. VII B, a prediction method of the stationary state is discussed and its results are compared with the simulation results. The paper is concluded in Sec. VIII.

II. THE PROPOSED KINETIC MODEL

We consider a fluid system composed of innumerable molecules confined in a spatially periodic domain, the unit cell of which is denoted by D . The behavior of the system is described by the following kinetic equation:

$$\frac{\partial f}{\partial t} + \xi_i \frac{\partial f}{\partial X_i} + F_i \frac{\partial f}{\partial \xi_i} = Q_c[f] + Q_d[f], \quad (1a)$$

$$Q_c[f] = A(\rho)(f_c - f), \quad A(\rho) > 0, \quad (1b)$$

$$Q_d[f] = -\frac{\partial}{\partial \xi_i} \{(\alpha_i + c_i \beta) f\}, \quad \mathbf{c} = \boldsymbol{\xi} - \mathbf{v}, \quad (1c)$$

$$F_i = -\frac{\partial \phi}{\partial X_i}, \quad \phi = \Phi_S(\rho, T) + \Phi_L[\rho], \quad (1d)$$

$$\alpha_i = \left(\frac{1}{\rho} \int \Phi_T d\rho \right) \frac{\partial T}{\partial X_i}, \quad \Phi_T = \frac{\partial \Phi_S}{\partial T}, \quad (1e)$$

$$\beta = \frac{1}{3\rho R} \left\{ \frac{\partial}{\partial t} \int \Phi_T d\rho + \frac{\partial}{\partial X_i} \left(v_i \int \Phi_T d\rho \right) \right\}, \quad (1f)$$

$$f_c = \frac{\rho}{(2\pi RT)^{3/2}} \exp\left(-\frac{c^2}{2RT}\right), \quad (1g)$$

$$\rho = \int f d\xi, \quad v_i = \frac{1}{\rho} \int \xi_i f d\xi, \quad (1h)$$

$$T = \frac{1}{3\rho R} \int c^2 f d\xi, \quad (1i)$$

where t is a time, \mathbf{X} and $\boldsymbol{\xi}$ are, respectively, a position and a molecular velocity ($\xi = |\boldsymbol{\xi}|$ will be used as well later), $f(t, \mathbf{X}, \boldsymbol{\xi})$ is the VDF of molecules, $m\mathbf{F}$ is a potential force acting on a single molecule with m and ϕ being the molecular mass and the potential, and $R = k_B/m$ with k_B being the Boltzmann constant. The potential ϕ is further split into Φ_S and Φ_L . They may be regarded, respectively, as a non-impulsive short-range (or localized) and long-range effect of molecular interactions. Unlike the previous model [14,15], the isothermal assumption is no longer made; accordingly, the present Φ_S is supposed to depend on T as well as on ρ . This feature and the new form of the collision effect are the main differences from the previous model. The density ρ , flow velocity \mathbf{v} , and temperature T are defined as the moment of f . Here and in what follows, the integral with respect to $\boldsymbol{\xi}$ represents the definite one over its whole space and that with respect to ρ is the one from 0 to ρ along the isothermal process, unless otherwise stated. The right-hand side of (1a) represents the intermolecular *collision* effect composed of two parts Q_c and Q_d . The first part, Q_c , is a familiar Bhatnagar-Gross-Krook (BGK)-type term [20], except for a generalized density dependence $A(\rho)$ to be specified later, and preserves the mass, momentum, and energy. The second part, Q_d , is a new part, the form of which is chosen in accordance with the external force term on the left-hand side of (1a) for modeling the nonimpulsive aspect of the repulsive interaction effect in cooperation with Φ_S and is related to it through the definitions of α_i and β ; see (1c), (1e), and (1f). The following properties of Q_d are readily obtained:

$$\langle Q_d[f] \rangle = 0, \quad \langle \xi_j Q_d[f] \rangle = \rho \alpha_j, \quad (2a)$$

$$\langle \frac{1}{2} \xi^2 Q_d[f] \rangle = v_i \rho \alpha_i + 3\beta \rho RT, \quad (2b)$$

where $\langle \bullet \rangle = \int \bullet d\xi$. In (1), distinct brackets $\langle \bullet \rangle$ and $[\bullet]$ are used. The round brackets represent the argument of a function, while the square brackets represent that of a functional or an operator. The reason for the form of α_i and β in (1e) and (1f) will become clear in Sec. III in the connection to the balance equations of momentum and energy.

As mentioned above, the self-consistent force potential ϕ is eventually split into the long-range part Φ_L and the short-range part Φ_S , along the same line of argument as in Refs. [14,15]. By use of the long-range intermolecular attractive potential $m\Psi$, the part Φ_L is expressed as

$$m\Phi_L(t, \mathbf{X}) = \int_{\mathbb{R}^3} \Psi(|\mathbf{Y} - \mathbf{X}|) \{ \rho(t, \mathbf{Y}) - \rho(t, \mathbf{X}) \} d\mathbf{Y}, \quad (3)$$

while the subtracted part $\{ \int_{\mathbb{R}^3} \Psi(|\mathbf{Y} - \mathbf{X}|) d\mathbf{Y} \} \rho(t, \mathbf{X})$ is combined with a repulsive potential part Φ_R to form the short-range part Φ_S in the total self-consistent potential ϕ :

$$m\Phi_S = m\Phi_R + \left\{ \int_{\mathbb{R}^3} \Psi(|\mathbf{Y} - \mathbf{X}|) d\mathbf{Y} \right\} \rho(t, \mathbf{X}). \quad (4)$$

The specific form of Φ_S will be determined later from the van der Waals equation of state in Sec. III A. The present splitting strategy is the same as that taken in the construction of the previous model.

When Ψ decays fast in the system size as usually expected, the variation of ρ is moderate and the Taylor expansion is allowed in the molecular-size scale [21] as in the previous model. The result is that

$$\Phi_L(t, \mathbf{X}) \simeq \frac{1}{6m} \int_{\mathbb{R}^3} \Psi(|\mathbf{r}|) |\mathbf{r}|^2 d\mathbf{r} \frac{\partial^2 \rho}{\partial X_i^2} \equiv -\kappa \frac{\partial^2 \rho}{\partial X_i^2}. \quad (5)$$

Note that $\kappa > 0$, since Ψ is attractive. This approximation is called the diffuse-interface model in the literature [22] and has been recently derived by Giovangigli [13] in getting the capillary fluid equations from the Enskog–Vlasov system, where the truncation of the Taylor expansion at the second-order derivative has also been employed.

III. BALANCE EQUATIONS AND FLUID-DYNAMIC QUANTITIES

By a few manipulations after taking 1, ξ_j , and ξ^2 moments of (1a), the set of balance equations is obtained:

$$\frac{\partial \rho}{\partial t} + \frac{\partial \rho v_i}{\partial X_i} = 0, \quad (6)$$

$$\frac{\partial \rho v_j}{\partial t} + \frac{\partial}{\partial X_i} \{ \rho v_i v_j + \langle c_i c_j f \rangle \} + \rho \frac{\partial \phi}{\partial X_j} = \rho \alpha_j, \quad (7)$$

$$\begin{aligned} \frac{\partial}{\partial t} \left[\frac{1}{2} \langle \mathbf{c}^2 f \rangle + \frac{1}{2} \rho v^2 \right] + \frac{\partial}{\partial X_i} \left[\left\{ \frac{1}{2} \langle \mathbf{c}^2 f \rangle + \frac{1}{2} \rho v^2 \right\} v_i \right. \\ \left. + \frac{1}{2} \langle c_i \mathbf{c}^2 f \rangle + \langle c_i c_j f \rangle v_j \right] + \rho v_i \frac{\partial \phi}{\partial X_i} \\ = \rho v_\ell \alpha_\ell + 3\beta \rho RT, \end{aligned} \quad (8)$$

where (2) has been taken into account. It is seen that (6) is the conservation equation of mass.

In what follows, in addition to $\Phi_T = \partial \Phi_S / \partial T$, we shall use the following short notations for the derivatives of $\Phi_S(\rho, T)$:

$$\Phi_\rho = \frac{\partial \Phi_S}{\partial \rho}, \quad \Phi_{\rho T} = \frac{\partial^2 \Phi_S}{\partial \rho \partial T}, \quad \Phi_{TT} = \frac{\partial^2 \Phi_S}{\partial T^2}.$$

A. Momentum equation

To identify the specific form of Φ_S , the balance equation of momentum (7) and the van der Waals equation of state will be used in a way similar to but slightly extended from that in Ref. [14]. Bearing in mind that the isothermal assumption is no longer made, the term related to Φ_S in ϕ is transformed as follows:

$$\begin{aligned} \rho \frac{\partial \Phi_S}{\partial X_j} &= \rho \left(\Phi_\rho \frac{\partial \rho}{\partial X_j} + \Phi_T \frac{\partial T}{\partial X_j} \right) \\ &= \frac{\partial}{\partial X_j} \int \rho \Phi_\rho d\rho + \int \Phi_T d\rho \frac{\partial T}{\partial X_j}. \end{aligned}$$

Remember that the integration with respect to ρ is taken from zero to ρ under the isothermal process, unless otherwise stated. Thanks to the definition (1e) of α_i , plugging the above

into (7) yields

$$\frac{\partial \rho v_j}{\partial t} + \frac{\partial}{\partial X_i} \left(\rho v_i v_j + \langle c_i c_j f \rangle + \int \rho \Phi_\rho d\rho \delta_{ij} \right) + \rho \frac{\partial \Phi_L}{\partial X_j} = 0.$$

Thus, the balance equation of momentum takes a familiar form of the momentum equation by defining the static pressure p and the stress tensor p_{ij} as

$$p = \frac{1}{3} \langle \mathbf{c}^2 f \rangle + \int \rho \Phi_\rho d\rho = \rho RT + \int \rho \Phi_\rho d\rho, \quad (9a)$$

$$p_{ij} = \langle c_i c_j f \rangle + \int \rho \Phi_\rho d\rho \delta_{ij}. \quad (9b)$$

In the meantime, the equation of state of the van der Waals fluid is given by

$$p = \frac{\rho RT}{1 - b\rho} - a\rho^2, \quad (10)$$

where a and b are positive constants. With the same b , the following form of $A(\rho)$ in the BGK-type term will be supposed:

$$A(\rho) = \frac{A_c \rho}{1 - b\rho}, \quad (11)$$

where A_c is a positive constant (see Appendix A). By comparing (10) with (9a), the specific forms of Φ_S and related quantities are identified as

$$\int \rho \Phi_\rho d\rho = \frac{\rho RT}{1 - b\rho} - \rho RT - a\rho^2, \quad (12a)$$

$$\Phi_\rho = \frac{b(2 - b\rho)}{(1 - b\rho)^2} RT - 2a, \quad (12b)$$

$$\begin{aligned} \Phi_S &= \int \Phi_\rho d\rho \\ &= RT \left\{ -\ln(1 - b\rho) + \frac{b\rho}{1 - b\rho} \right\} - 2a\rho, \end{aligned} \quad (12c)$$

$$\Phi_T = R \left\{ -\ln(1 - b\rho) + \frac{b\rho}{1 - b\rho} \right\}, \quad (12d)$$

$$\int \Phi_T d\rho = -\rho R \ln(1 - b\rho), \quad (12e)$$

$$\Phi_{\rho T} = \frac{bR(2 - b\rho)}{(1 - b\rho)^2}, \quad (12f)$$

$$\int \rho \Phi_{\rho T} d\rho = \frac{b\rho^2 R}{1 - b\rho}, \quad \Phi_{TT} = 0. \quad (12g)$$

Note that, except for Φ_ρ and $\Phi_{\rho T}$, they vanish in the low density limit $\rho \rightarrow 0$.

In the rest of the paper, the fact that Φ_T and $\Phi_S - T\Phi_T$ are independent of T will be used, sometimes without notice, for simplifying calculations. If the cubic equation of state such as Peng–Robinson and Soave–Redlich–Kwong [23] is adopted in place of the van der Waals equation of state, Φ_T and $\Phi_S - T\Phi_T$ become no longer independent of T and, accordingly, some calculations, especially those in the variational analysis in Sec. V, become complicated. Moreover, the transformation of β from (1f) to (16) that appears later is not allowed. Nevertheless, the monotone property of H_p to be discussed in Sec. IV, which is the crucial property in the

present model, is unchanged. In this sense, the present model approach is applicable to the fluids obeying other equations of state.

B. Energy equation

Finally, a reduction of the equation of energy balance will be considered. Before starting, it is necessary to introduce a thermodynamically consistent definition of the specific internal energy e . According to the thermodynamics, the specific internal energy e is related to the pressure p as

$$e = \int \rho^{-2} \left(p - T \frac{\partial p}{\partial T} \right) d\rho + \frac{3}{2} RT.$$

In the above expression, the independent variables of the function p are ρ and T , and the integration with respect to ρ is taken under the isothermal process. Since p is defined by (9a), the above equation is recast into

$$\begin{aligned} e &= \int \rho^{-2} \left\{ \int \rho \Phi_{\rho} d\rho - T \int \rho \Phi_{\rho T} d\rho \right\} d\rho + \frac{3}{2} RT \\ &= \rho^{-1} \left\{ \int \Phi_S d\rho - T \int \Phi_T d\rho \right\} + \frac{3}{2} RT \end{aligned}$$

or, equivalently,

$$\rho e = \frac{1}{2} \langle c^2 f \rangle + \int \Phi_S d\rho - T \int \Phi_T d\rho, \quad (13)$$

by using the definition of T in (1).

Bearing in mind the above definition, let us turn to the energy balance. With the aid of the mass conservation and the relation $\rho \Phi_S = \int \rho \Phi_{\rho} d\rho + \int \Phi_S d\rho$ obtained by the integration by parts, the term related to Φ_S is eventually transformed into

$$\begin{aligned} \rho v_i \frac{\partial \Phi_S}{\partial X_i} &= \frac{\partial}{\partial X_i} \left[\left(\int \rho \Phi_{\rho} d\rho + \int (\Phi_S - T \Phi_T) d\rho \right) v_i \right] \\ &\quad + \frac{\partial}{\partial t} \int (\Phi_S - T \Phi_T) d\rho \\ &\quad + T \frac{\partial}{\partial t} \left(\int \Phi_T d\rho \right) + \frac{\partial}{\partial X_i} \left(v_i T \int \Phi_T d\rho \right). \end{aligned}$$

Note that, because of (1e) and (1f),

$$T \frac{\partial}{\partial t} \left(\int \Phi_T d\rho \right) + \frac{\partial}{\partial X_i} \left(v_i T \int \Phi_T d\rho \right) = 3\rho RT \beta + \rho v_i \alpha_i,$$

and that the contribution from the Q_d term is canceled out. Hence, the energy balance (8) is transformed into

$$\begin{aligned} &\frac{\partial}{\partial t} \left[\frac{1}{2} \langle c^2 f \rangle + \int (\Phi_S - T \Phi_T) d\rho + \frac{1}{2} \rho v^2 \right] \\ &\quad + \frac{\partial}{\partial X_i} \left[\left\{ \frac{1}{2} \langle c^2 f \rangle + \int \rho \Phi_{\rho} d\rho + \int (\Phi_S - T \Phi_T) d\rho \right. \right. \\ &\quad \left. \left. + \frac{1}{2} \rho v^2 \right\} v_i + \frac{1}{2} \langle c_i c^2 f \rangle + \langle c_i c_j f \rangle v_j \right] \\ &\quad + \rho v_i \frac{\partial \Phi_L}{\partial X_i} = 0, \end{aligned}$$

which is rewritten in the form

$$\begin{aligned} &\frac{\partial}{\partial t} \left[\rho \left(e + \frac{1}{2} v^2 \right) \right] + \frac{\partial}{\partial X_i} \left[\rho \left(e + \frac{1}{2} v^2 \right) v_i \right. \\ &\quad \left. + \frac{1}{2} \langle c_i c^2 f \rangle + p_{ij} v_j \right] + \frac{\partial \Phi_L}{\partial X_i} \rho v_i = 0, \end{aligned}$$

with the aid of the expressions of the stress tensor (9b) and of the internal energy (13). By simply defining the heat flow q_i as

$$q_i = \frac{1}{2} \langle c_i c^2 f \rangle,$$

the familiar form of energy equation is recovered.

C. Summary

In summary, the familiar form of the mass conservation, the momentum, and the energy equation has been recovered:

$$\frac{\partial}{\partial t} \rho + \frac{\partial}{\partial X_i} (\rho v_i) = 0, \quad (14a)$$

$$\frac{\partial}{\partial t} (\rho v_j) + \frac{\partial}{\partial X_i} (\rho v_i v_j + p_{ij}) + \rho \frac{\partial \Phi_L}{\partial X_j} = 0, \quad (14b)$$

$$\frac{\partial}{\partial t} \left[\rho \left(e + \frac{1}{2} v^2 \right) \right] + \frac{\partial}{\partial X_i} \left[\rho \left(e + \frac{1}{2} v^2 \right) v_i \right] \quad (14c)$$

$$+ q_i + p_{ij} v_j \Big] + \rho v_i \frac{\partial \Phi_L}{\partial X_i} = 0, \quad (14d)$$

with the following definitions of pressure, internal energy, stress tensor, and heat-flow vector:

$$p = \frac{1}{3} \langle c^2 f \rangle + \int \rho \Phi_{\rho} d\rho, \quad (15a)$$

$$\rho e = \frac{1}{2} \langle c^2 f \rangle + \int (\Phi_S - T \Phi_T) d\rho, \quad (15b)$$

$$p_{ij} = \langle c_i c_j f \rangle + \int \rho \Phi_{\rho} d\rho \delta_{ij}, \quad q_i = \frac{1}{2} \langle c_i c^2 f \rangle. \quad (15c)$$

The nonideal gas effect occurs in the above definitions as the integration terms of Φ_S and its derivatives.

In the case of the van der Waals fluid, Φ_T is independent of T as seen from (12), and the time derivative term of Φ_T in the definition of β can be transformed into a spatial derivative with the aid of the mass conservation as

$$\beta = \frac{1}{3\rho R} \left(\int \Phi_T d\rho - \rho \Phi_T \right) \frac{\partial v_i}{\partial X_i}. \quad (16)$$

Remember that the specific forms of Φ_S and its related quantities have been identified as well, see (12). Accordingly, α_i and β also depend on the parameters a and b in the van der Waals equation of state through Φ_S . Incidentally, the κ defined in the diffuse-interface approximation (5) for Φ_L has a close connection with the parameter a through the attractive intermolecular potential Ψ . Namely, comparing (4) with (12c) gives

$$a = -\frac{1}{2m} \int_{\mathbb{R}^3} \Psi(|r|) dr,$$

while κ in (5) is defined as

$$\kappa = -\frac{1}{6m} \int_{\mathbb{R}^3} |r|^2 \Psi(|r|) dr.$$

In the rest of the paper, κ and a will be treated as independent parameters, reflecting the degree of freedom on the choice of Ψ .

Finally, it should be noted that the term containing Φ_L is responsible for the interface creation between two phases. Its effect in the stationary state will be demonstrated and briefly discussed later in Sec. VII in the case of the diffuse-interface approximation (5). Incidentally, (14) with (15) is not a closed system. It can be made closed only in the fluid-dynamic limit. By the standard asymptotic analyses, say the Hilbert or the Chapman-Enskog expansion, one should obtain the constitutive equations for the stress tensor and the heat flow, which is not discussed in the present paper.

IV. H THEOREM AND MINIMIZATION PROBLEM

In the present section, a functional that is monotonic in time is shown to exist for the proposed model.

As in the usual step to derive the Boltzmann H theorem [3], integrate (1a) multiplied by $1 + \ln(f/c_0)$ over the whole space of ξ , where c_0 is a constant having the same physical dimension as f . Then, after a few manipulations, the following identity is obtained:

$$\begin{aligned} & \frac{\partial}{\partial t} \left\langle f \ln \frac{f}{c_0} \right\rangle + \frac{\partial}{\partial X_i} \left\langle \xi_i f \ln \frac{f}{c_0} \right\rangle \\ &= A(\rho, T) \left\langle f_e \left(1 - \frac{f}{f_e} \right) \ln \frac{f}{f_e} \right\rangle - 3\beta\rho. \end{aligned}$$

In the above, the first and the second term on the right-hand side come from Q_c and Q_d , respectively. Note that the first term is nonpositive. Then, the substitution of (1f) leads to

$$\begin{aligned} & \frac{\partial}{\partial t} \left\{ \left\langle f \ln \frac{f}{c_0} \right\rangle + \frac{1}{R} \int \Phi_T d\rho \right\} \\ &+ \frac{\partial}{\partial X_i} \left\{ \left\langle \xi_i f \ln \frac{f}{c_0} \right\rangle + \frac{v_i}{R} \int \Phi_T d\rho \right\} \\ &= A(\rho, T) \left\langle f_e \left(1 - \frac{f}{f_e} \right) \ln \frac{f}{f_e} \right\rangle \leq 0, \quad (17) \end{aligned}$$

where the equality condition for the last inequality is that $f = f_e$. Therefore, if the domain is periodic, the following inequality holds:

$$\frac{d}{dt} H_p \equiv \frac{d}{dt} \int_D \left\{ \left\langle f \ln \frac{f}{c_0} \right\rangle + \frac{1}{R} \int \Phi_T d\rho \right\} dX \leq 0. \quad (18)$$

This means that H_p monotonically decreases in time and that f becomes the local Maxwellian f_e in the stationary state. In other words, the minimizer of the present minimization problem is the Maxwellian. If the kinetic extension of the specific entropy s is defined as

$$\rho s = -R \left\langle f \ln \frac{f}{c_0} \right\rangle - \int \Phi_T d\rho, \quad (19)$$

it recovers the thermodynamically consistent expression based on the relation $de = Tds - pd(1/\rho)$ in the local equilibrium

state:

$$s = -R \ln(\rho T^{-3/2}) - (1/\rho) \int \Phi_T d\rho + \text{const}. \quad (20)$$

Hence, H_p may be interpreted as a kinetic extension of the negative total entropy. Similarly, the kinetic extension of the specific Gibbs energy g may be defined based on the thermodynamic relation as

$$g = e - Ts + p/\rho = \frac{5}{2}RT + \Phi_S + \frac{RT}{\rho} \left\langle f \ln \frac{f}{c_0} \right\rangle. \quad (21)$$

It leads to the following familiar expression in the local equilibrium state:

$$g = \frac{5}{2}RT + \Phi_S + T \{ R \ln(\rho T^{-3/2}) + \text{const} \}. \quad (22)$$

The minimization problem in the case of the domain surrounded by the isothermal wall is discussed in Appendix B.

V. PRELIMINARY ANALYSES

In the present section and numerical simulations, the approximation (5) for Φ_L will be used. However, in the manipulations that apply to the original form of Φ_L as well, the notation Φ_L will be retained.

Before going into detail, it should be noted that there are five conservative quantities. To see it, integrate the mass, the momentum, and the energy equation with respect to X over the domain D . Then it is found that

$$\begin{aligned} & \frac{\partial}{\partial t} \int_D \rho dX = 0, \\ & \frac{\partial}{\partial t} \int_D \rho v_j dX + \int_D \rho \frac{\partial}{\partial X_j} \Phi_L dX = 0, \\ & \frac{\partial}{\partial t} \int_D \left[\rho \left(e + \frac{1}{2} v^2 \right) \right] dX + \int_D \rho v_i \frac{\partial}{\partial X_i} \Phi_L dX = 0. \end{aligned}$$

Irrespective of whether the original definition or the approximation (5) is taken for Φ_L , it can be shown that $\int_D \rho \partial_j \Phi_L dX = 0$ and $\int_D \{ \rho v_i \partial \Phi_L / \partial X_i - (1/2) \partial(\rho \Phi_L) / \partial t \} dX = 0$ [24]. Using these relations, it is immediate to see that the following quantities are constant in time:

$$C_0 = \int_D \rho dX, \quad (23a)$$

$$C_i = \int_D \rho v_i dX \quad (i = 1, 2, 3), \quad (23b)$$

$$C_4 = \int_D \left[\rho \left(e + \frac{1}{2} v^2 + \frac{1}{2} \Phi_L \right) \right] dX. \quad (23c)$$

The constants C_0 , C_i , and C_4 represent the total mass, momentum, and energy, respectively.

A. Stationary state

Consider first the variational problem for H_p under the above total mass, momentum, and energy constraints. To this

end, consider

$$\begin{aligned} \mathcal{H}_p[f; \lambda_0, \lambda_1, \lambda_2, \lambda_3, \lambda_4] &= H_p[f] + \lambda_0 \left\{ \int_D \rho d\mathbf{X} - C_0 \right\} \\ &+ \lambda_i \left\{ \int_D \rho v_i d\mathbf{X} - C_i \right\} \\ &+ \lambda_4 \left\{ \int_D \rho \left(e + \frac{1}{2} \mathbf{v}^2 + \frac{1}{2} \Phi_L \right) d\mathbf{X} - C_4 \right\}, \end{aligned}$$

where λ_0 , λ_i , and λ_4 are the Lagrangian multipliers. Its first variation $\delta\mathcal{H}_p$ is then written as

$$\begin{aligned} \delta\mathcal{H}_p &= \delta H_p + \lambda_0 \int_D \delta\rho d\mathbf{X} + \lambda_i \int_D \delta(\rho v_i) d\mathbf{X} \\ &+ \lambda_4 \delta \int_D \left\{ \rho \left(e + \frac{1}{2} \mathbf{v}^2 + \frac{1}{2} \Phi_L \right) \right\} d\mathbf{X}. \end{aligned}$$

Note that $\delta\rho = \langle \delta f \rangle$ and $\delta(\rho v_i) = \langle \xi_i \delta f \rangle$. By using the identity $\int_D \rho \Phi_L[\delta\rho] d\mathbf{X} = \int_D \Phi_L[\rho] \delta\rho d\mathbf{X}$ [25], it is eventually transformed into

$$\begin{aligned} \delta\mathcal{H}_p &= \int_D \left\{ \left\langle \ln \frac{f}{c_0} + 1 + \frac{1}{R} \Phi_T + \lambda_0 + \lambda_i \xi_i \right. \right. \\ &\left. \left. + \lambda_4 \left(\frac{1}{2} \xi^2 + \Phi_S - T \Phi_T + \Phi_L[\rho] \right) \right\} \delta f d\mathbf{X}, \end{aligned}$$

where the fact that $\Phi_S - T\Phi_T$ is independent of T has been used. Thus, in the stationary state, it holds that

$$\begin{aligned} f &= c_0 \exp \left(-\frac{\lambda_4}{2} \left\{ \xi_i + \frac{\lambda_i}{\lambda_4} \right\}^2 + \frac{\lambda_i^2}{2\lambda_4} \right. \\ &\left. - 1 - \frac{1}{R} \Phi_T - \lambda_0 - \lambda_4 (\Phi_S - T\Phi_T + \Phi_L[\rho]) \right). \end{aligned}$$

It is now clear that f is a Maxwellian in the stationary state. Moreover, λ 's are expressed with the aid of the definitions of ρ , ρv_i , and T as

$$\begin{aligned} \lambda_4 &= \frac{1}{RT}, \quad \lambda_i/\lambda_4 = -v_i, \\ c_0 \exp \left(\frac{\lambda_i^2}{2\lambda_4} - 1 - \frac{1}{R} \Phi_T - \lambda_0 \right. \\ &\left. - \lambda_4 (\Phi_S - T\Phi_T + \Phi_L[\rho]) \right) = \frac{\rho}{(2\pi RT)^{3/2}}. \end{aligned}$$

The equations on the first line tell that T and v_i are constant, and the last equation is reduced to

$$\begin{aligned} c_0 (2\pi RT)^{3/2} \exp \left(\frac{v_i^2}{2RT} - 1 - \lambda_0 \right) \\ = \rho \exp \left(\frac{\Phi_S + \Phi_L[\rho]}{RT} \right). \end{aligned} \quad (24)$$

Therefore, $\rho \exp(\frac{\Phi_S + \Phi_L[\rho]}{RT})$ is constant as well in the stationary state. In particular, any uniform equilibrium state is a stationary state.

B. Stability of the uniform equilibrium state against small disturbances

Next study the local stability of the uniform equilibrium state. Since the uniform equilibrium state is a stationary state of the functional \mathcal{H}_p , its stability for small deviations can be studied by the second variation of \mathcal{H}_p ; see, e.g., Ref. [26]. Since ρ and $\rho\mathbf{v}$ are linear moments of f , the second and third terms of \mathcal{H}_p do not contribute to the second variation. $\delta^2\mathcal{H}_p$ is then written as

$$\delta^2\mathcal{H}_p = \delta^2 H_p + \lambda_4 \delta^2 \int_D \left\{ \rho \left(e + \frac{1}{2} \mathbf{v}^2 + \frac{1}{2} \Phi_L \right) \right\} d\mathbf{X}.$$

After some manipulations, the above equation is eventually reduced to

$$\delta^2\mathcal{H}_p = \int_D \left\{ \left\langle \frac{1}{f} (\delta f)^2 \right\rangle + \frac{\Phi_\rho(\delta\rho)^2 + \Phi_L[\delta\rho]\delta\rho}{RT} \right\} d\mathbf{X},$$

where $\lambda_4 = 1/RT$ has been taken into account. Again, the fact that $\Phi_S - T\Phi_T$ is independent of T has been used. By the Cauchy–Schwartz inequality, $\langle \delta f \rangle^2 = \langle (\delta f/\sqrt{f})\sqrt{f} \rangle^2 \leq \langle (\delta f)^2/f \rangle \langle f \rangle$, so that $(\delta\rho)^2 \leq \rho \langle (\delta f)^2/f \rangle$, where the equality holds only when $(\delta f)/f = \text{const}$. Moreover, it can be shown that $\int_D \Phi_L[\delta\rho]\delta\rho d\mathbf{X} \geq 0$, so that

$$\delta^2\mathcal{H}_p \geq \int_D \left(\frac{1}{\rho} + \frac{\Phi_\rho}{RT} \right) (\delta\rho)^2 d\mathbf{X}.$$

Bearing in mind that the uniform equilibrium state is a stationary state, the necessary condition for the uniform equilibrium state with density ρ_0 , temperature T_0 , and velocity \mathbf{v}_0 to be stable for any *small* disturbances is given by [27]

$$\frac{1}{\rho_0} + \frac{\Phi_\rho(\rho_0, T_0)}{RT_0} > 0, \quad (25a)$$

which is eventually reduced to

$$a < \frac{RT_0}{2\rho_0(1 - b\rho_0)^2}. \quad (25b)$$

The bound of the above condition,

$$c \left(\equiv \frac{a}{bRT_0} \right) = \frac{1}{2b\rho_0(1 - b\rho_0)^2}, \quad (26)$$

becomes critical in the limit $\int_D \Phi_L[\delta\rho]\delta\rho d\mathbf{X} \rightarrow 0$ or $\kappa \rightarrow 0$. The conditions (25) and (26) derived above are essentially the same as those for the previous model in Ref. [15], if T_0 is regarded as the temperature T_* of the thermal bath in that model.

In the meantime, the above stability criteria should be obtained by the linear stability analysis, as was done in Ref. [15] for the previous model. However, the required calculation becomes by far more cumbersome than the previous model, which motivates us to take the above different approach. In spite of such a difficulty, a simplification method of the linear stability analysis can be found in Ref. [28] for the Enskog–Vlasov system with a special form of *correlation* factor for the two-particle distribution function. To follow the method, first linearize the stationary state (24) around the uniform state with the density ρ_0 and temperature T_0 , and then put the density perturbation in the form $\exp(i\mathbf{k} \cdot \mathbf{X})$, namely, focus on the *frozen wave*, the perturbation with zero growth. Just for

simplicity, let us consider Φ_L of the form (5) here. Then it is eventually obtained that

$$\frac{\kappa}{2} |k|^2 = a - \frac{RT_0}{2\rho_0(1-b\rho_0)^2}. \quad (27)$$

According to Benilov and Benilov [28], the existence of a positive frozen wave mode is the indicator of instability, namely, the state satisfying $a > \frac{RT_0}{2\rho_0(1-b\rho_0)^2}$ should have unstable modes. Then, the same stability criterion as (26) is obtained. However, it should be remarked as in Ref. [15] that the present linear stability analysis does not take into account the period of domain; thus, when applied to the periodic domain, there are forbidden areas of mode near $|k| = 0$. We will come back later to this issue in the first paragraph of Sec. VII A 2 with numerical examples. Incidentally, Ref. [28] further discussed the solid/fluid transition based on the frozen mode investigation. Since we do not intend to reproduce the solidification by the present model, we do not proceed further here.

C. Metastable state

In Sec. VB, the stability of the uniform state against *small* disturbances has been discussed by the second variation, and the explicit form of the neutral curve (26) in the case $\Phi_L \rightarrow 0$ or $\kappa \rightarrow 0$ has been obtained. However, the uniform state may be unstable for *large* disturbances, even if it is stable against small ones, and is accordingly called metastable. This issue is discussed in the present subsection. Additional discussions will be given in Sec. VII B.

The analyses in Sec. VA show that the stationary state is characterized as the local equilibrium state f_e with the uniform velocity $\mathbf{v} = \mathbf{C}/C_0$ and the uniform temperature T , and T is determined through the total energy conservation that eventually takes the following form:

$$C_4 = \frac{3}{2}RTC_0 + \frac{1}{2}\frac{C^2}{C_0} + \int_D \left\{ \int (\Phi_S - T\Phi_T)d\rho + \frac{1}{2}\rho\Phi_L[\rho] \right\} dX. \quad (28)$$

Moreover, the substitution of such a stationary state into the original kinetic equation gives the following identities:

$$\begin{aligned} \frac{1}{\rho} \frac{\partial \rho}{\partial X_i} + \frac{1}{RT} \left(\frac{\partial \Phi_S}{\partial X_i} + \frac{\partial \Phi_L[\rho]}{\partial X_i} \right) &= 0, \\ \frac{1}{\rho} \frac{\partial \rho}{\partial t} - \frac{v_i}{RT} \left(\frac{\partial \Phi_S}{\partial X_i} + \frac{\partial \Phi_L[\rho]}{\partial X_i} \right) &= 0. \end{aligned}$$

It should be remarked that these are identical to the stationary condition (24) that has already been derived in Sec. VA. Indeed, combining these, it is seen that

$$\frac{\partial \rho}{\partial t} + v_i \frac{\partial \rho}{\partial X_i} = 0,$$

saying that the density profile is conveyed by the fluid motion, without changing its shape in the stationary state (v_i is constant in the stationary state). Moreover, the first equation

can be transformed in two different ways: One is

$$\begin{aligned} \frac{\partial}{\partial X_i} \left(\ln \rho + \frac{\Phi_S + \Phi_L[\rho]}{RT} \right) &= 0, \\ \Leftrightarrow \frac{\partial}{\partial X_i} (g + \Phi_L[\rho]) &= 0, \end{aligned} \quad (29)$$

which is equivalent to the stationary condition (24) [see (22) for the form of g at the local equilibrium], and the other is

$$\begin{aligned} \frac{\partial}{\partial X_i} (\rho RT) + \rho \left(\frac{\partial \Phi_S}{\partial X_i} + \frac{\partial \Phi_L[\rho]}{\partial X_i} \right) &= 0, \\ \Rightarrow \frac{\partial}{\partial X_i} \left(\rho RT + \int \rho \Phi_\rho d\rho \right) + \rho \frac{\partial \Phi_L[\rho]}{\partial X_i} &= 0, \\ \Leftrightarrow \frac{\partial}{\partial X_i} p + \rho \frac{\partial \Phi_L[\rho]}{\partial X_i} &= 0. \end{aligned} \quad (30)$$

Equations (29) and (30) are identical as a differential equation, but g and p are different as a function of ρ . When Φ_L is negligible, they imply that the specific Gibbs energy g and the static pressure p are both spatially uniform; the classical phase equilibrium condition in thermodynamics [29,30] is recovered.

Motivated by this observation, let us consider the stationary state established after a long-time evolution from the uniform equilibrium state with density ρ_0 , flow velocity \mathbf{v}_0 , and temperature T_0 . The state is initially disturbed in such a way that the total density, momentum, and energy in the system are unchanged. Then,

$$\begin{aligned} C_0 &= \rho_0 L^3, \quad \mathbf{C} = C_0 \mathbf{v}_0, \\ C_4 &= \frac{3}{2}RT_0 C_0 + \frac{1}{2}\frac{C^2}{C_0} + L^3 \int_0^{\rho_0} (\Phi_S - T\Phi_T)d\rho, \end{aligned}$$

where L^3 is the volume of domain and (28) is reduced to

$$\begin{aligned} T &= T_0 - \frac{2}{3} \frac{1}{R\rho_0 L^3} \int_D \left\{ \int_0^\rho (\Phi_S - T\Phi_T)d\rho \right. \\ &\quad \left. + \frac{1}{2}\rho\Phi_L[\rho] \right\} dX. \end{aligned} \quad (31)$$

Here it is used that $\Phi_S - T\Phi_T$ depends only on ρ . Since $\int_D \int_0^\rho (\Phi_S - T\Phi_T)d\rho dX = -a \int_D (\rho - \rho_0)^2 dX \leq 0$ and $\int_D \rho\Phi_L[\rho]dX \geq 0$, (31) says that, once the phase transition takes place, the attractive molecular interaction part of the internal energy is released and spent on the temperature raise and the interface creation.

As will be shown in numerical simulations, the uniform equilibrium state changes to a new stationary state, which has plateaux with higher density, say ρ_A , and with lower density, say ρ_B , in the density profile, unless the uniform state is stable against the initial disturbance. Moreover, under the approximation $\Phi_L = -\kappa \partial^2 \rho / \partial X_i^2$, as κ tends to zero, the interface connecting plateaux becomes thinner and finally turns into a discontinuity, so the volume fraction of the plateaux can be defined without ambiguity. Let χ_A denote the volume fraction of the plateau with density ρ_A in such a situation. Then the mass conservation is reduced to

$$\rho_0 = \rho_A \chi_A + \rho_B (1 - \chi_A), \quad (32)$$

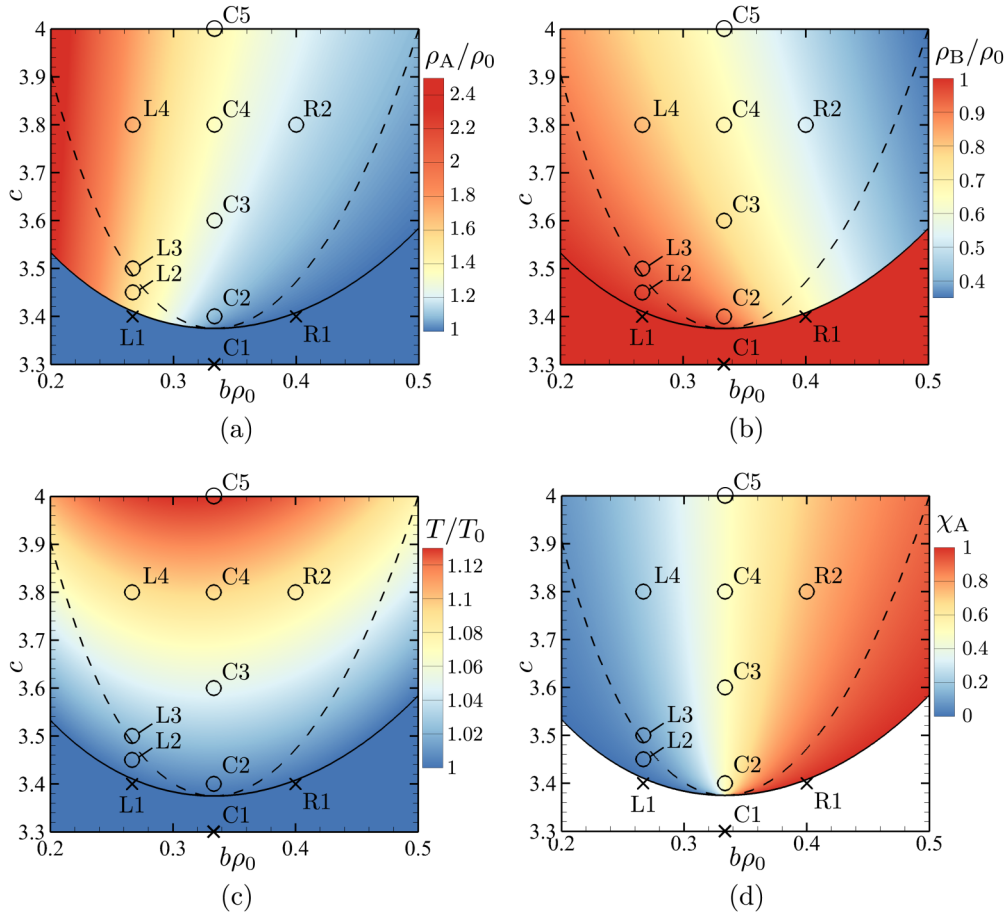


FIG. 1. The density, temperature, and volume fraction in the stationary state in the limit $\kappa \rightarrow 0$. (a) ρ_A , (b) ρ_B , (c) T , and (d) χ_A . The dashed line indicates the curve (26), while the solid line the curve (35). The symbols (\circ or \times) with the label C1, L1, R1, etc. indicate the cases where the numerical simulation has been carried out.

and (29) and (30) are reduced to [31]

$$g(\rho_A, T) = g(\rho_B, T), \quad p(\rho_A, T) = p(\rho_B, T). \quad (33)$$

Since the contribution of $\rho\Phi_L$ vanishes [32], (31) is reduced to

$$\begin{aligned} T &= T_0 - \frac{2}{3} \frac{1}{R\rho_0 L^3} \int_D \left\{ \int_{\rho_0}^{\rho} (\Phi_S - T\Phi_T) d\rho \right\} dX \\ &= T_0 + \frac{2}{3} \frac{a}{R\rho_0} \{ \chi_A (\rho_A - \rho_0)^2 \\ &\quad + (1 - \chi_A) (\rho_B - \rho_0)^2 \} \\ &= T_0 + \frac{2}{3} \frac{a}{R\rho_0} (\rho_A - \rho_0) (\rho_0 - \rho_B). \end{aligned} \quad (34)$$

Hence there are four equations [(32)–(34)]—enough to determine four constants χ_A , ρ_A , ρ_B , and T —that characterize the new stationary state in the limit $\kappa \rightarrow 0$. Such a transition to the new stationary state takes place in a certain (not the entire) region of (a, b) . On the bound of that region, the volume fraction of one of the plateaux vanishes, because only a single state (or initial uniform equilibrium state) is allowed outside of the bound. Hence, the bound can be found by taking the limit $\chi_A \rightarrow 0$ or $\chi_A \rightarrow 1$, which corresponds to $\rho_B \rightarrow \rho_0$ or

$\rho_A \rightarrow \rho_0$, respectively. Then, by (34), $T \rightarrow T_0$ and (33) is solved to give

$$\begin{aligned} g\left(\frac{1 - b\rho_0}{2b} + \frac{1}{2b} \sqrt{(1 + b\rho_0)^2 - \frac{4bRT_0}{a(1 - b\rho_0)}}, T_0\right) \\ = g(\rho_0, T_0), \end{aligned} \quad (35a)$$

for $1/3 < b\rho_0 < 1$ and

$$\begin{aligned} g\left(\frac{1 - b\rho_0}{2b} - \frac{1}{2b} \sqrt{(1 + b\rho_0)^2 - \frac{4bRT_0}{a(1 - b\rho_0)}}, T_0\right) \\ = g(\rho_0, T_0), \end{aligned} \quad (35b)$$

for $0 \leq b\rho_0 < 1/3$. The set of equations (35) represents the curve of the bound, i.e., the relation between a and b in the limit $\kappa \rightarrow 0$; see Appendix C for the derivation. Figure 1 shows the map of ρ_A , ρ_B , T , and χ_A thus obtained. The curves (26) and (35) are overplotted in the same figure. It is clearly seen that the density, which plays a role of the *order parameter* here, changes abruptly across the curve (35), which is in marked contrast with its smooth change across the curve (26).

It should also be noted that the temperature in the stationary states after the phase transition is different from T_0 , as seen in Fig. 1(c). This is due to the physical system

under consideration being thermodynamically isolated. In other words, the system under consideration is thermodynamically different from the previous model [14,15], even though the previous model gives essentially the same stability criterion. The change of temperature will affect the densities of two phases that emerge after the phase transition. The details will be discussed in Appendix D.

VI. DIMENSIONLESS DESCRIPTION AND THE CHARACTERISTIC PARAMETERS

Let us introduce the following notation:

$$\begin{aligned} t &= L(2RT_0)^{-1/2}\tilde{t}, & X_i &= Lx_i, & \xi_i &= (2RT_0)^{1/2}\zeta_i, \\ \rho &= \rho_0\tilde{\rho}, & T &= T_0\tilde{T}, & v_i &= (2RT_0)^{1/2}\tilde{v}_i, \\ f &= \frac{\rho_0}{(2RT_0)^{3/2}}\tilde{f}, & c_0 &= \rho_0(2\pi RT_0)^{-3/2}, \\ \phi &= 2RT_0\tilde{\phi}, & \Phi_S &= 2RT_0\tilde{\Phi}_S, & \Phi_L &= 2RT_0\tilde{\Phi}_L, \\ \Psi &= (2RT_0/(\rho_0L^3))\tilde{\Psi}, & \kappa &= (2RT_0L^2/\rho_0)\tilde{\kappa}, \\ a &= \tilde{a}RT_0/\rho_0, & b &= \tilde{b}/\rho_0, & \tilde{c}_i &= \zeta_i - \tilde{v}_i, \\ A(\rho) &= A(\rho_0)\tilde{A}(\tilde{\rho}), & Q_d[f] &= \frac{\rho_0}{2RT_0L}\tilde{Q}_d[\tilde{f}]. \end{aligned}$$

Then,

$$\begin{aligned} \tilde{A} &= \frac{1-\tilde{b}}{1-\tilde{b}\tilde{\rho}}\tilde{\rho}, & \tilde{\rho} &= \int \tilde{f}d\zeta, & \tilde{v}_i &= \frac{1}{\tilde{\rho}}\int \zeta_i\tilde{f}d\zeta, \\ \tilde{T} &= \frac{2}{3\tilde{\rho}}\int \tilde{c}^2\tilde{f}d\zeta, & \tilde{Q}_d[\tilde{f}] &= -\frac{\partial}{\partial\zeta_i}(\tilde{f}\tilde{g}_i), \\ \tilde{g}_i &= \frac{1}{\tilde{\rho}}\int \tilde{\Phi}_{\tilde{T}}d\tilde{\rho}\frac{\partial\tilde{T}}{\partial x_i} - \frac{2}{3\tilde{\rho}}\int \tilde{\rho}\tilde{\Phi}_{\tilde{T}}d\tilde{\rho}\frac{\partial\tilde{v}_k}{\partial x_k}\tilde{c}_i, \end{aligned}$$

where

$$\begin{aligned} \tilde{\Phi}_S &= \frac{1}{2}\left\{-\ln(1-\tilde{b}\tilde{\rho}) + \frac{\tilde{b}\tilde{\rho}}{1-\tilde{b}\tilde{\rho}}\right\}\tilde{T} - \tilde{a}\tilde{\rho}, \\ \int \tilde{\Phi}_{\tilde{T}}d\tilde{\rho} &= -\frac{1}{2}\tilde{\rho}\ln(1-\tilde{b}\tilde{\rho}), \\ \int \tilde{\rho}\tilde{\Phi}_{\tilde{T}}d\tilde{\rho} &= \frac{1}{2}\frac{\tilde{b}\tilde{\rho}^2}{1-\tilde{b}\tilde{\rho}}, \\ \tilde{\Phi}_L(\mathbf{x}) &= \int \tilde{\Psi}(|\tilde{\mathbf{r}}|)\{\tilde{\rho}(\mathbf{x}+\tilde{\mathbf{r}}) - \tilde{\rho}(\mathbf{x})\}d\tilde{\mathbf{r}} \\ &\text{or} = -\tilde{\kappa}\frac{\partial^2\tilde{\rho}}{\partial x_i^2} \\ \text{with } \tilde{\kappa} &= -\frac{2}{3}\pi\int_0^\infty \tilde{\Psi}(\tilde{r})\tilde{r}^4d\tilde{r}, \end{aligned}$$

and the original equation is reduced to

$$\frac{\partial\tilde{f}}{\partial\tilde{t}} + \zeta_i\frac{\partial\tilde{f}}{\partial x_i} - \frac{\partial\tilde{\phi}}{\partial x_i}\frac{\partial\tilde{f}}{\partial\zeta_i} = \frac{2}{\sqrt{\pi}}\frac{1}{\text{Kn}}\tilde{Q}_c[\tilde{f}] + \tilde{Q}_d[\tilde{f}], \quad (36)$$

where

$$\begin{aligned} \tilde{Q}_c[\tilde{f}] &= \tilde{A}(\tilde{\rho})(\tilde{f}_e - \tilde{f}), & \tilde{f}_e &= \frac{\tilde{\rho}}{(\pi\tilde{T})^{3/2}}\exp\left(-\frac{\tilde{c}^2}{\tilde{T}}\right), \\ \tilde{\phi} &= \tilde{\Phi}_S(\tilde{\rho}) + \tilde{\Phi}_L, \end{aligned}$$

and Kn is the *Knudsen number* defined by

$$\text{Kn} = \frac{(8RT_0/\pi)^{1/2}}{A(\rho_0)L}.$$

As is clear from the above, the present fluid system is characterized by the following parameters: \tilde{a} , \tilde{b} , $\tilde{\kappa}$, and Kn. In place of this set of parameters, we shall use $c \equiv \tilde{a}/\tilde{b} [= a/(bRT_0)]$, $\tilde{b} (= b\rho_0)$, $K \equiv \tilde{\kappa}/\tilde{b}$, and $k \equiv (\sqrt{\pi}/2)\text{Kn}$ as the independent parameters in the presentation of numerical simulations in Sec. VII.

One may find some similarity of (36) to the kinetic equation with chemical reactions in the sense that Kn occurs only in front of \tilde{Q}_c ; see, e.g., Refs. [33,34]. Here, \tilde{Q}_d and a part of $\partial\tilde{\Phi}_S/\partial x_i$ may be thought to represent the effects of repulsive interactions of a nonimpulsive nature between molecules.

VII. NUMERICAL SIMULATIONS: RESULTS AND DISCUSSIONS

The numerical simulations are planned under the setting that the state is periodic in x_1 and is uniform in the other two spatial directions under the approximation $\tilde{\Phi}_L = -\tilde{\kappa}\partial^2\tilde{\rho}/\partial x_1^2$. Each simulation starts by disturbing the uniform equilibrium state at rest with density ρ_0 and temperature T_0 to make it another local Maxwellian at rest with the following density ρ_{ini} and temperature T_{ini} :

$$\begin{aligned} \frac{\rho_{\text{ini}}}{\rho_0} &= 1 + \epsilon_\rho \sin(2\pi X_1/L), \\ \frac{T_{\text{ini}}}{T_0} &= 1 + \frac{2}{3}\frac{1}{R\rho_0T_0L}\int_0^L \left\{ a(\rho_{\text{ini}} - \rho_0)^2 + \frac{1}{2}\rho_{\text{ini}}\kappa\frac{\partial^2\rho_{\text{ini}}}{\partial X_1^2} \right\} dX_1. \end{aligned}$$

The form of the above temperature comes from the specified density disturbance as the consequence of the total energy constraint (31).

Numerically studied are cases $(\tilde{b}, c) = (1/3, 3.3)$, $(1/3, 3.4)$, $(1/3, 3.6)$, $(1/3, 3.8)$, $(1/3, 4.0)$, $(4/15, 3.4)$, $(4/15, 3.45)$, $(4/15, 3.5)$, $(4/15, 3.8)$, $(2/5, 3.4)$, and $(2/5, 3.8)$, which will be labeled as case C1, C2, C3, C4, C5, L1, L2, L3, L4, R1, and R2, respectively. For each case, the other parameters k , K , and ϵ_ρ in the initial disturbance are set variously, according to the purpose of computations. Cases C1–R2 above are shown in each panel of Fig. 1. In the figure, the open circle indicates the case where the phase transition took place at least for one set of values of k , K , and ϵ_ρ , while the cross symbol indicates the case where the transition was not observed.

A. Results

In cases C1, L1, and R1, which are all below the curve (35), the phase transition was not observed at all for different values of K and ϵ_ρ ; the disturbance decreases and the uniform equilibrium state is recovered. In contrast, in cases C2–C5, L2–L4, and R2, which are all above the curve (35), the phase transition was observed, at least for a certain set of values of K and ϵ_ρ . As an example, the time evolution process of the phase transition for case C4 is shown in Fig. 2. It is observed that the disturbance develops to establish a new stationary state with two plateaux of density; the temperature becomes uniform but not the same as T_{ini} nor T_0 . As is already explained just below

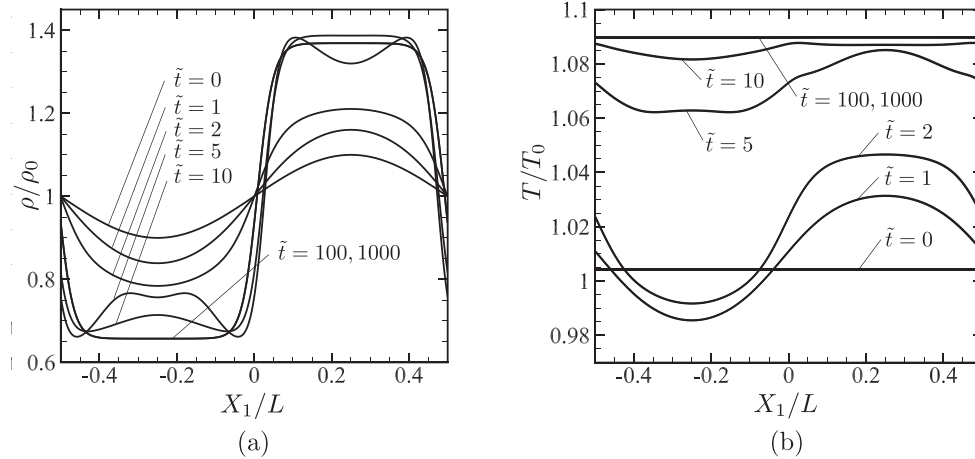


FIG. 2. Time evolution of the density and temperature: Case C4 with $K = 1.0 \times 10^{-4}$, $k = 0.1$, and $\epsilon_\rho = 0.1$. (a) Density and (b) temperature.

(31), the increase of temperature in Fig. 2(b) is due to the release of attractive intermolecular force energy in the internal energy. Since K is small, the released energy is mostly spent on the temperature raise (nearly by 10%), not on the interface creation.

1. The stable, the metastable, and the unstable region

Next let us show the cases close to the curves (26) and (35). Cases L1, L2, and L3 belong, respectively, to the stable, the metastable, and the unstable region in the limit $K \rightarrow 0$. Figures 3 and 4 show the results for these cases in the case of $K = 1.0 \times 10^{-5}$ and $k = 0.1$. In case L2, which locates between the two curves (26) and (35) in Fig. 1, the disturbance decreases for a very small disturbance with $\epsilon_\rho = 0.01$, while it grows for the disturbance with $\epsilon_\rho = 0.1$. In the latter, the initially dense spot becomes the nucleus that triggers the nucleation, the characteristic process expected in the metastable region, see Fig. 3(b). In case L1, even for a very large disturbance with $\epsilon_\rho = 0.9$, the phase transition does not occur, suggesting that the uniform equilibrium state is stable, see Fig. 4(a). In case L3, on the contrary, even a very small distur-

bance with $\epsilon_\rho = 0.01$ causes the phase transition, suggesting that the uniform state is unstable, see Fig. 4(b). Because K is very small, the theoretical consequences in the limit $K \rightarrow 0$ in Secs. VB and VC well predict the occurrence of the phase transition.

2. Influence of K and the Knudsen number

Although the results for $K = 1.0 \times 10^{-5}$ agree well with the consequences in Secs. VB and VC, some discrepancies are found as K increases. Indeed, as shown in Fig. 5(a), when $K = 1.0 \times 10^{-4}$, even for a very large disturbance with $\epsilon_\rho = 0.9$, the phase transition does not occur in case L2, although case L2 is above the curve (35). Another example is found in case L3, which is above the curve (26), where the phase transition ceases to occur even for a very large disturbance with $\epsilon_\rho = 0.9$ when $K = 1.0 \times 10^{-3}$, see Fig. 5(b). These results suggest that the stable region extends upward in the $\tilde{b}c$ plane as K increases, see Fig. 1. Judging from (27) and the last paragraph of Sec. V in Ref. [15], this is due to the simulations being performed in the periodic domain. Since small but nonzero modes have wavelengths that are too

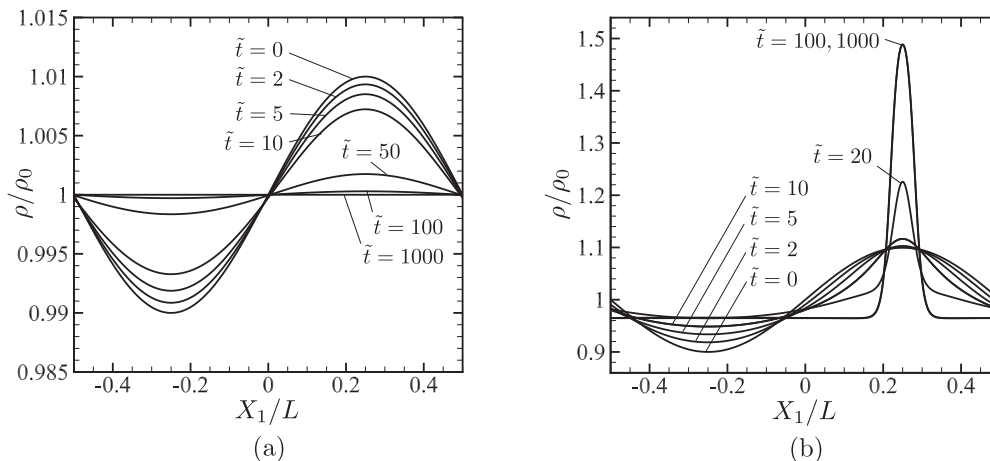


FIG. 3. Time evolution of the density: Case L2 with $K = 1.0 \times 10^{-5}$ and $k = 0.1$ from different initial disturbances. (a) $\epsilon_\rho = 0.01$ and (b) $\epsilon_\rho = 0.1$.

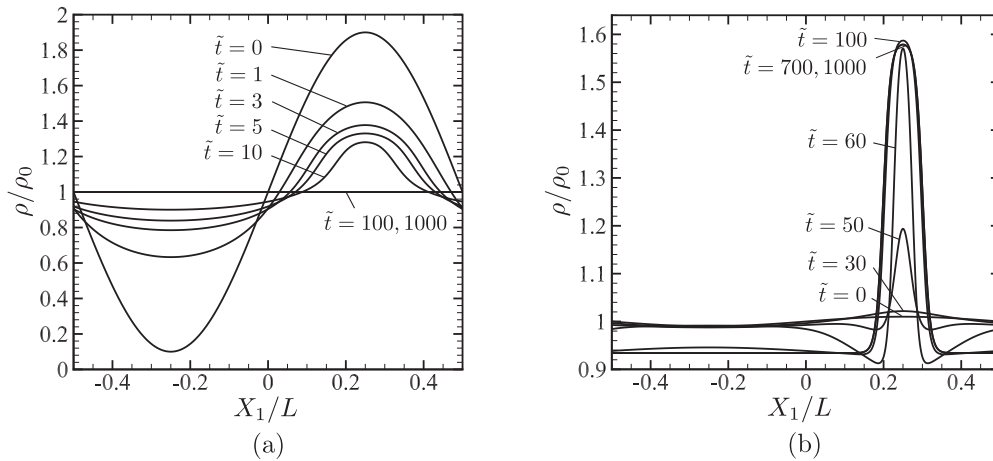


FIG. 4. Time evolution of the density for large and small disturbances. (a) Case L1 with $\epsilon_\rho = 0.9$ and (b) case L3 with $\epsilon_\rho = 0.01$. The other parameters are commonly set as $K = 1.0 \times 10^{-5}$ and $k = 0.1$.

long and are not compatible with the periodic condition, they are excluded. It explains why the criterion may depend on K (or κ).

The influence of K appears as well in the cases enough above the curve (26). It was observed that, as K becomes smaller, features of higher frequency modes appear in the time evolution process and the interface becomes thinner. Moreover, the temperature rises more from its initial value as K becomes smaller. (Compare Fig. 2 with Figs. S.1 and S.2 in Supplemental Material (SM) [35].) It is due to less energy being spent on the interface creation because of its small thickness [32]. The close observation on the temperature based on the energy consideration is one of the merits of the present model over the previous simple model. The influence of the temperature change in phase transition is discussed in detail in the Appendix D.

Finally, the influence of the Knudsen number on the transient process was also examined in case C4 with $K = 1.0 \times 10^{-4}$ and $k = 0.005, 0.01$, and 1 . The result for the same K with $k = 0.1$ has already been shown in Fig. 2. Comparisons

of the results show that the stationary state is not affected by the difference of k . However, k affects the duration of time required to reach the stationary state: the time duration becomes longer for smaller k . Moreover, the transient process becomes more complicated for smaller k . (Compare Fig. 2 with Fig. S.3 in the SM [35].)

Before closing the simulation result presentation, the information of computations is briefly described. The actual computations are carried out, after a uniform discretization both in the spatial and the velocity space, by a semi-Lagrangian method with a uniform time interval $\Delta\tilde{t}$. The typical setting of computational parameters is the combination of 640 uniform intervals both in the spatial and the velocity space, where the velocity space is truncated at $\zeta_1 = \pm 6$, and $\Delta\tilde{t} = 5 \times 10^{-5}$ and mostly gives satisfactory results. There are, however, some exceptions that required much finer intervals in space, velocity, and time. The results shown in the present paper are those for which the numerical convergence has been judged within the error invisible in the figures.

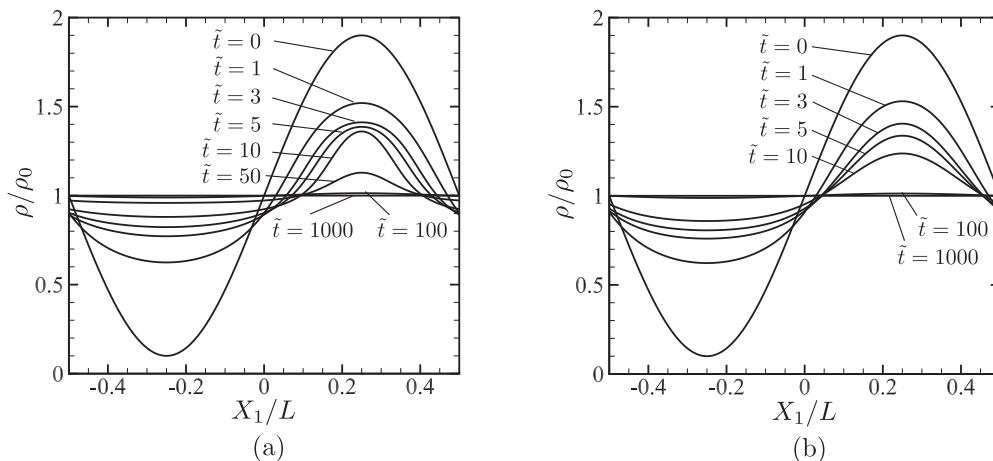


FIG. 5. Time evolution of the density: Cases L2 and L3. (a) Case L2 with $K = 1.0 \times 10^{-4}$, $k = 0.1$, and $\epsilon_\rho = 0.9$. (b) Case L3 with $K = 1.0 \times 10^{-3}$, $k = 0.1$, and $\epsilon_\rho = 0.9$.

B. Discussions

As presented in Sec. VII A, the density plateaux are eventually established after a long time as the final stationary state, when the uniform state is not stable against the initial disturbance. That stationary state can be, however, predicted by the set of Eqs. (29), (30), and (31) without solving the kinetic equation directly. The method of prediction is explained below in referring the preliminary analyses in Sec. V C.

In the one-dimensional case, Eqs. (29), (30), and (31) are reduced to

$$\kappa \frac{\partial^2 \rho}{\partial X_1^2} = g - g_A = g - g_B, \quad (37a)$$

$$p - \rho \kappa \frac{\partial^2 \rho}{\partial X_1^2} + \frac{\kappa}{2} \left(\frac{\partial \rho}{\partial X_1} \right)^2 = p_A = p_B, \quad (37b)$$

$$T = T_0 + \frac{2}{3} \frac{1}{R \rho_0 L} \int_D \left\{ a(\rho^2 - \rho_0^2) + \frac{\kappa}{2} \rho \frac{\partial^2 \rho}{\partial X_1^2} \right\} dX_1, \quad (37c)$$

where the quantities with the subscripts A and B denote their values at the individual plateaux. The following iterative procedure is adopted to predict the stationary state:

- (1) Put $T = T_0$ as the initial guess of T .
- (2) Solve $g_A = g_B$ and $p_A = p_B$ to get ρ_A and ρ_B . Then get the temporal value of χ_A by using (32).
- (3) Set the origin of the coordinate X_1 so that $\rho(0) = \rho_{\sharp}$, where $\rho_{\sharp} = (\rho_A + \rho_B)/2$. By eliminating $\partial^2 \rho / \partial X_1^2$ from (37a) and (37b), another condition at $X_1 = 0$ is obtained as

$$\left. \frac{\partial \rho}{\partial X_1} \right|_{\sharp} = \sqrt{\frac{2}{\kappa} \{ p_A - p_{\sharp} + \rho_{\sharp} (g_{\sharp} - g_A) \}}, \quad (38)$$

where the quantities with the subscript \sharp denote their values at $X_1 = 0$.

- (4) Then using (38) and $\rho(0) = \rho_{\sharp}$ as the set of boundary conditions, solve (37a) to get ρ from $X = 0$ in the positive and the negative direction, respectively, say, by the Successive Over-Relaxation (SOR) method. The plateau ρ_A will appear on the positive side, while the plateau ρ_B will appear on the negative side of X_1 .

- (5) Integrate the obtained density over a half period, from $X_1 = -(1 - \chi_A)L/2$ to $X_1 = \chi_A L/2$, and compute

$$\Delta C_0 = \rho_0 L - 2 \int_{-(1-\chi_A)L/2}^{\chi_A L/2} \rho dX_1,$$

$$\Delta \chi_A = \frac{\Delta C_0}{(\rho_A - \rho_B)L}.$$

Then update χ_A by $\Delta \chi_A$, so that the constraint of the total mass is fulfilled. The density over one period is obtained by $\rho(X)$ in $(-(L/2)(1 - \chi_A), (L/2)\chi_A]$ and $\rho(\chi_A L - X)$ in $((L/2)\chi_A, (L/2)(1 + \chi_A)]$.

- (6) Put $D = (-(L/2)(1 - \chi_A), (L/2)(1 + \chi_A)]$ and update T by (37c).

- (7) Go back to the step 2 until the appropriate convergence criterion is fulfilled.

Practically, step 6 requires a certain relaxation skill in updating T for the stable numerical computation.

The results of the prediction method above are compared with the stationary states obtained by the numerical simula-

tions of the kinetic equation in Fig. 6. Excellent agreement is achieved, even in Fig. 6(c) where the formation of the higher density plateau is not sufficient. Since the Knudsen number is not involved in the present prediction method, the excellent agreement explains why the final stationary states were not affected by k in the simulations; see Fig. S.3 in the SM [35].

VIII. CONCLUSION

In the present paper, we propose a kinetic model for the phase transition of the van der Waals fluid. The model is constructed as follows:

- (1) As was done in the previous simple model, the short-range interaction represented by Φ_S is determined to be consistent with the van der Waals equation of state.

- (2) To get rid of the isothermal assumption in the previous model, the new collision effect Q_d is introduced. Its form is determined so that the momentum and the energy conservation are assured.

- (3) The collision frequency $A(\rho)$ in the BGK-type collision term Q_c is determined to recover the leading order part of the viscosity obtained from the Enskog equation. Consequently, the real gas effect is introduced in Q_c as well.

For the new model, the H theorem holds. The stability of the uniform equilibrium state and the stationary state to be established after a long time are discussed in detail. The following qualitative features are clarified.

- (1) There is a monotonically decreasing function H_p . This function takes a different form from the counterpart of the previous model with the isothermal assumption and may be interpreted as a kinetic extension of the negative entropy of the fluid system.

- (2) In the stationary state, the VDF is the local Maxwellian with the uniform temperature and velocity. That Maxwellian is determined by the constraints of the total mass, momentum, and energy (23) and the stationary condition (24) [or (29)]. Moreover, the thus-determined state recovers the phase equilibrium condition in thermodynamics, i.e., the temperature, static pressure, and specific Gibbs free energy are common to two phases, in the limit $\kappa \rightarrow 0$.

- (3) By the procedure given in Sec. VII B, it is possible to predict the local Maxwellian at the final stationary state without directly solving the kinetic equation. It is also suggested from the prediction in the limit $\kappa \rightarrow 0$ (Fig. 1) that the parameter \tilde{b} largely affects the volume fraction χ_A , while c largely affects the temperature.

- (4) The sufficient condition for the uniform equilibrium state to be stable or meta-stable is (26). It becomes a necessary condition as well in the limit $\kappa \rightarrow 0$. Hence (26) is the so-called spinodal line in the conventional thermodynamics, while (35) is the so-called binodal line. The latter coincides with the bound of the coexisting state or the bound between the metastable and the stable region in the limit $\kappa \rightarrow 0$.

- (5) For a given uniform equilibrium state, its stability and the final stationary state depend only on a , b , and κ , not on the Knudsen number.

Finally, the numerical simulations for spatially one-dimensional periodic domain are performed. The approximation (5) for Φ_L is employed, supposing that the attractive part of the intermolecular potential decays fast in the scale of the

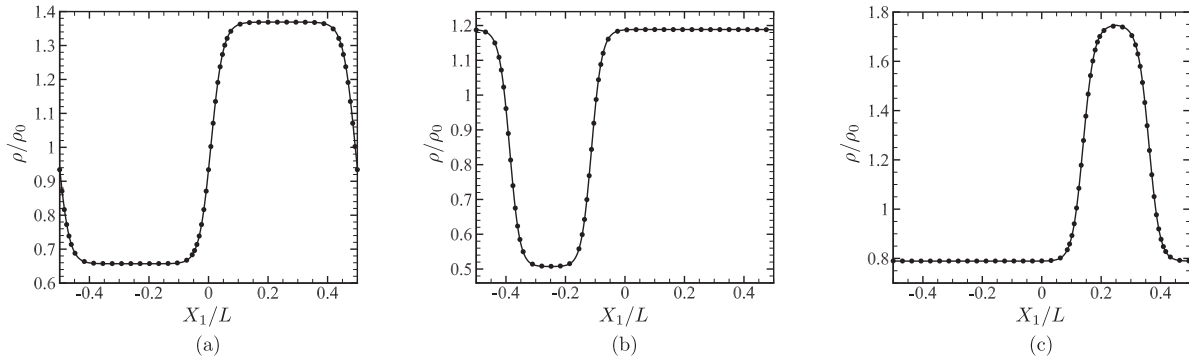


FIG. 6. Comparisons of density profile between the simulation and the prediction result. (a) Case C4, (b) case R2, and (c) case L4. Here K is commonly put as $K = 1.0 \times 10^{-4}$. The solid line indicates the prediction result, while the bullets the simulation result. The prediction result is shifted to adjust the position of the interface with the simulation result.

period of domain under consideration. The following results are obtained.

(1) The numerical simulations confirm the existence of the unstable, the metastable, and the stable uniform equilibrium state. In the first two cases, the phase transition is induced even by a small disturbance and only by a large disturbance, respectively. In the last case, the transition is not induced even by a large disturbance.

(2) As K increases, the stable region in the (\tilde{b}, c) diagram becomes larger, while the unstable region becomes smaller. Moreover, K affects the transient process toward the stationary state; for smaller K , features of higher frequency modes appear and the process becomes more complicated. The interface thickness in the stationary state is also affected by K ; it becomes thinner for smaller K .

(3) The Knudsen number also affects the transient process toward the stationary state but not the stability and the final stationary state. In the simulations for $k < 1$, it is observed that the time duration to reach the stationary state becomes longer and the transient process appears more complicated for smaller k .

ACKNOWLEDGMENTS

The present work was supported in part by JSPS KAKENHI Grant No. 17K18840.

APPENDIX A: ON THE FORM OF $A(\rho)$

In the literature, the equation of state of a hard-sphere dense gas is given as [36]

$$p = \rho RT \left(1 + \frac{2\pi}{3} \sigma^3 \frac{\rho}{m} \chi \right),$$

where σ is a diameter of a molecule and χ is a density-dependent factor required to be unity in the low density limit $\rho \rightarrow 0$. Since there are no attracting forces among hard-sphere molecules, there is no counterpart of the parameter a occurring in the van der Waals equation in the above equation of state. Then, it is seen that there is the following correspondence of quantities:

$$\frac{2\pi}{3} \sigma^3 \frac{\rho}{m} \chi = \frac{b\rho}{1 - b\rho}.$$

To have the consistent second virial coefficient,

$$b = \frac{2\pi}{3} \frac{\sigma^3}{m},$$

is required as well. Hence, it follows that

$$\chi = \frac{1}{1 - b\rho}.$$

In the meantime, by the standard Chapman–Enskog method [5] or Hilbert method [3], the viscosity μ is expressed as $\mu = RT/A(\rho)$ for the present model. For the Enskog equation, μ is related to the counterpart of the rarefied gas μ_0 as

$$\mu\chi = \mu_0,$$

at the leading order of expansion with respect to $\phi\chi$, where $\phi = \pi\rho\sigma^3/(6m)$ [1,36]. Hence, it is appropriate to put

$$A(\rho) = \frac{A_c\rho}{1 - b\rho}.$$

Incidentally, as in the literature on the original BGK model, A_c can be extended to be a positive function of T . In that case, it is appropriate to denote it as $A(\rho, T) = A_c(T)\rho/(1 - b\rho)$.

APPENDIX B: SUPPLEMENTAL DISCUSSIONS ON THE CASE SURROUNDED BY THE ISOTHERMAL SOLID WALL

When the domain is surrounded by the resting isothermal wall with temperature T_w , there are some subtle issues to be addressed on the proposed model.

First, in the definition of Φ_L , the integration with respect to \mathbf{Y} is no longer taken over the whole space \mathbb{R}^3 but within the domain D . Then, it becomes straightforward to show that $\int_D (\partial\rho/\partial t) \Phi_L d\mathbf{X} = (1/2)(\partial/\partial t) \int_D \rho \Phi_L d\mathbf{X}$, thanks to the domain of integration being common between \mathbf{X} and \mathbf{Y} , giving an additional symmetry for their exchange [37].

Second, the minimization problem needs additional considerations. Suppose that the conventional kinetic boundary condition [38] is applied on the wall, i.e.,

$$f(t, \mathbf{X}, \boldsymbol{\xi}) = \int_{\boldsymbol{\xi}' \cdot \mathbf{n} < 0} \mathcal{R}(\boldsymbol{\xi}' \rightarrow \boldsymbol{\xi}; t, \mathbf{X})$$

$$\times f(t, \mathbf{X}, \xi') \frac{|\xi' \cdot \mathbf{n}|}{|\xi \cdot \mathbf{n}|} d\xi', \quad \xi \cdot \mathbf{n} > 0.$$

Here \mathbf{n} is the unit normal of the boundary pointing to the gas side and \mathcal{R} is the reflection probability density such that

$$\begin{aligned} \int_{\xi \cdot \mathbf{n} > 0} \mathcal{R}(\xi' \rightarrow \xi; t, \mathbf{X}) d\xi &= 1, \quad \xi' \cdot \mathbf{n} < 0, \\ \mathcal{R}(\xi' \rightarrow \xi; t, \mathbf{X}) &\geq 0, \\ M_w(\xi) &= \int_{\xi' \cdot \mathbf{n} < 0} \mathcal{R}(\xi' \rightarrow \xi; t, \mathbf{X}) M_w(\xi') \frac{|\xi' \cdot \mathbf{n}|}{|\xi \cdot \mathbf{n}|} d\xi', \end{aligned}$$

where $M_w \equiv (2\pi RT_w)^{-3/2} \exp[-\xi^2/(2RT_w)]$ is the wall Maxwellian with unit density, and any other Maxwellian with unit density does not satisfy the boundary condition. Thus, the specular reflection is excluded from the present discussion. Then, the multiplication of (1a) by $1 + \ln(f/\rho_0 M_w)$ in place of $1 + \ln(f/c_0)$ does work, where ρ_0 is a certain reference density. After a few manipulations, the integration of the result over the whole space of ξ is transformed into

$$\begin{aligned} \frac{\partial}{\partial t} \left\langle f \ln \frac{f}{\rho_0 M_w} \right\rangle + \frac{\partial}{\partial X_i} \left\langle \xi_i f \ln \frac{f}{\rho_0 M_w} \right\rangle \\ + \frac{\partial \phi}{\partial X_i} \frac{\rho v_i}{RT_w} = A(\rho, T) \left\langle f_e \left(1 - \frac{f}{f_e} \right) \ln \frac{f}{f_e} \right\rangle \\ - 3\beta\rho + \frac{1}{RT_w} \{v_\ell \rho \alpha_\ell + 3\rho\beta RT\} \\ \leq -3\beta\rho + \frac{1}{RT_w} \{v_\ell \rho \alpha_\ell + 3\rho\beta RT\}, \end{aligned} \quad (\text{B1})$$

where the last equality holds only when $f = f_e$. In the meantime, because of the transformation

$$\begin{aligned} \frac{\partial \Phi_S}{\partial X_i} \rho v_i &= \frac{\partial}{\partial X_i} (\Phi_S \rho v_i) + \frac{\partial}{\partial t} \int \Phi_S d\rho \\ &\quad - \int \Phi_T d\rho \frac{\partial T}{\partial t}, \end{aligned}$$

(B1) is rewritten as

$$\begin{aligned} \frac{\partial}{\partial t} \left\{ \left\langle f \ln \frac{f}{\rho_0 M_w} \right\rangle + \frac{1}{RT_w} \int \Phi_S d\rho \right\} \\ + \frac{\partial}{\partial X_i} \left\{ \left\langle \xi_i f \ln \frac{f}{\rho_0 M_w} \right\rangle + \frac{\rho v_i \Phi_S}{RT_w} \right\} + \frac{\partial \Phi_L}{\partial X_i} \frac{\rho v_i}{RT_w} \\ \leq \frac{1}{RT_w} \int \Phi_T d\rho \frac{\partial T}{\partial t} - 3\rho\beta + \frac{\rho}{RT_w} (\alpha_\ell v_\ell + 3\beta RT). \end{aligned}$$

From (1e) and (1f), the right-hand side is eventually reduced to

$$\begin{aligned} \text{R.H.S.} &= \frac{1}{RT_w} \left\{ \frac{\partial}{\partial t} \left((T - T_w) \int \Phi_T d\rho \right) \right. \\ &\quad \left. + \frac{\partial}{\partial X_i} \left(v_i (T - T_w) \int \Phi_T d\rho \right) \right\}, \end{aligned}$$

and the following inequality is obtained with the aid of the mass conservation equation (6):

$$\frac{\partial}{\partial t} \mathcal{A} + \frac{\partial}{\partial X_i} \mathcal{A}_i + \frac{\Phi_L}{RT_w} \frac{\partial \rho}{\partial t} \leq 0, \quad (\text{B2})$$

where

$$\begin{aligned} \mathcal{A} &= \left\langle f \ln \frac{f}{\rho_0 M_w} \right\rangle + \frac{1}{RT_w} \int \Phi_S d\rho \\ &\quad - \frac{T - T_w}{RT_w} \int \Phi_T d\rho, \\ \mathcal{A}_i &= \left\langle \xi_i f \ln \frac{f}{\rho_0 M_w} \right\rangle + \frac{\rho v_i (\Phi_S + \Phi_L)}{RT_w} \\ &\quad - v_i \frac{T - T_w}{RT_w} \int \Phi_T d\rho. \end{aligned}$$

By the identity announced in the second paragraph of the Appendix B, the third term of (B2) is then incorporated with the first term, and the integration with respect to \mathbf{X} and applying the Gauss divergence theorem leads to

$$\begin{aligned} \frac{d}{dt} H_{\text{th}} &\equiv \frac{d}{dt} \int_D \left\{ \mathcal{A} + \frac{\rho \Phi_L}{2RT_w} \right\} d\mathbf{X} \\ &\leq \int_{\partial D} n_i \mathcal{A}_i dS = \int_{\partial D} \left\langle \xi_i n_i f \ln \frac{f}{\rho_0 M_w} \right\rangle dS \leq 0. \end{aligned} \quad (\text{B3})$$

Here two properties on the boundary have been used. Namely, the normal component of the flow velocity vanishes and the following Darrozes-Guiraud inequality [3,39] holds on the boundary,

$$\int \xi_i n_i f \ln f d\xi \leq \int \xi_i n_i f \ln(\rho_0 M_w) d\xi,$$

where the equality holds only when $f \propto \rho_0 M_w$. Hence, combining two equality conditions leads to the equality condition $f = \rho M_w$ for (B3). In conclusion,

$$H_{\text{th}} \equiv \int_D \left(\mathcal{A} + \frac{\rho \Phi_L}{2RT_w} \right) d\mathbf{X},$$

monotonically decreases in time in the system that is surrounded by the isothermal wall.

Incidentally, it should be noted that $\int_D \Psi(|\mathbf{Y} - \mathbf{X}|) d\mathbf{Y}$ may depend on \mathbf{X} in the vicinity of the boundary. Hence, the second term of the right-hand side of (4) does not necessarily match the assumption that Φ_S is a function of ρ and T . One possibility to avoid the inconsistency is to introduce the ansatz that Φ_R cancels out the undesired \mathbf{X} dependence. The other possibility is to keep the definition (4) unchanged and instead to change the definition of Φ_L slightly as

$$\begin{aligned} m\Phi_L(t, \mathbf{X}) &= \int_D \Psi(|\mathbf{Y} - \mathbf{X}|) \{ \rho(t, \mathbf{Y}) - \rho(t, \mathbf{X}) \} d\mathbf{Y} \\ &\quad - \int_{\mathbb{R}^3 \setminus D} \Psi(|\mathbf{Y} - \mathbf{X}|) d\mathbf{Y} \rho(t, \mathbf{X}). \end{aligned}$$

This modification of Φ_L , which is appreciable only near the boundary due to the rapid decay of Ψ , does not affect the transformation of the third term of (B2). The inequality (B3) still holds accordingly.

APPENDIX C: THE BOUND OF CO-EXISTING REGION

As announced in Sec. VC, the derivation of the bound of coexisting region is given in this Appendix.

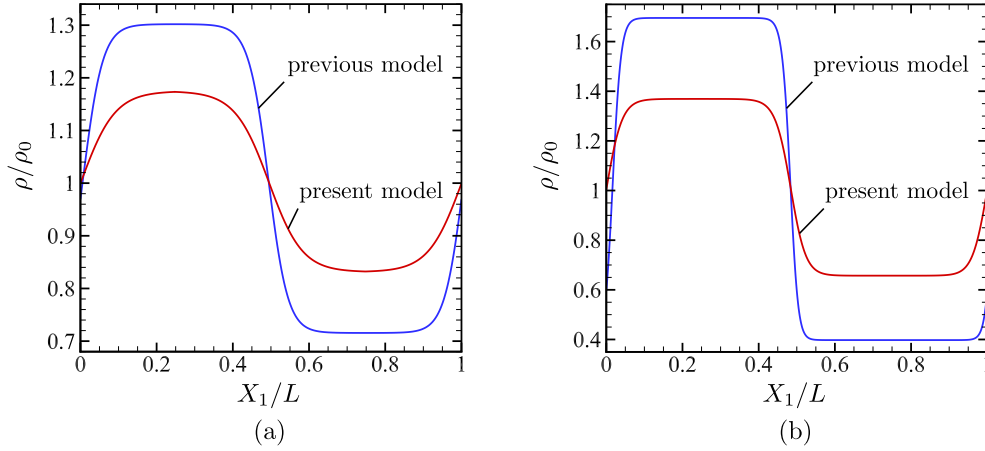


FIG. 7. Comparisons of the density profile in the stationary state between the previous and the present model. (a) Case C2 and (b) Case C4. In both cases, $K = 1.0 \times 10^{-4}$.

In the limit $\rho_A \downarrow \rho_0$ ($\chi_A \uparrow 1$) or $\rho_B \uparrow \rho_0$ ($\chi_A \downarrow 0$), one may put $T = T_0$ by (34) and, accordingly, the condition of the uniform static pressure is simplified as

$$\frac{\rho RT_0}{1 - b\rho} - a\rho^2 = \frac{\rho_0 RT_0}{1 - b\rho_0} - a\rho_0^2$$

and is solved for ρ as

$$\rho = \frac{1}{2b} \left\{ 1 - b\rho_0 \pm \sqrt{(1 + b\rho_0)^2 - \frac{4bRT_0}{a(1 - b\rho_0)}} \right\}.$$

The condition of the uniform specific Gibbs energy then takes the form [see (22)]

$$\begin{aligned} RT_0 \left(\ln \frac{b\rho}{1 - b\rho} + \frac{1}{1 - b\rho} \right) - 2a\rho \\ = RT_0 \left(\ln \frac{b\rho_0}{1 - b\rho_0} + \frac{1}{1 - b\rho_0} \right) - 2a\rho_0, \end{aligned}$$

which is eventually reduced to the condition

$$\mathcal{G}(\rho) = \mathcal{G}(\rho_0),$$

where

$$\mathcal{G}(\rho) \equiv \ln \frac{b\rho}{1 - b\rho} - \left(\frac{1}{1 - b\rho} + \frac{1}{1 - b\rho_0} \right) \frac{\rho - \rho_0}{\rho + \rho_0}.$$

It is readily seen that \mathcal{G} takes its maximum at $\rho_* \equiv (1 - b\rho_0)/(2b)$, because

$$\frac{d\mathcal{G}}{d\rho} = \frac{(\rho - \rho_0)^2(1 - 2b\rho - b\rho_0)}{\rho(1 - b\rho)^2(\rho + \rho_0)^2(1 - b\rho_0)}.$$

Hence, when $\rho_0 > \rho_*$, i.e., $b\rho_0 > 1/3$, the solution for $\mathcal{G}(\rho) = \mathcal{G}(\rho_0)$ is smaller than ρ_* and represents ρ_B , while the solution is larger than ρ_* and represents ρ_A when $b\rho_0 < 1/3$.

When $b\rho_0 = 1/3$, there is no difference between ρ_A and ρ_B and they take the common value of ρ_0 . Thus, on the bound of region of the coexisting states:

$$\begin{aligned} \rho_A &= \rho_* + \frac{1}{2b} \sqrt{(1 + b\rho_0)^2 - \frac{4bRT_0}{a(1 - b\rho_0)}}, \\ \rho_B &= \rho_0, \end{aligned} \quad (C1a)$$

for $0 \leq b\rho_0 < \frac{1}{3}$,

$$\rho_A = \rho_B = \rho_0, \quad (C1b)$$

for $b\rho_0 = \frac{1}{3}$, and

$$\begin{aligned} \rho_B &= \rho_* - \frac{1}{2b} \sqrt{(1 + b\rho_0)^2 - \frac{4bRT_0}{a(1 - b\rho_0)}}, \\ \rho_A &= \rho_0, \end{aligned} \quad (C1c)$$

for $\frac{1}{3} < b\rho_0 < 1$. These expressions, in turn, give the relation between a and b on the bound of the coexisting region, once substituted to $\mathcal{G}(\rho_A) = \mathcal{G}(\rho_0)$ when $0 \leq b\rho_0 < 1/3$ and to $\mathcal{G}(\rho_B) = \mathcal{G}(\rho_0)$ when $1/3 < b\rho_0 < 1$. It is the solid line shown in Fig. 1.

APPENDIX D: COMPARISONS WITH THE PREVIOUS MODEL

As mentioned at the end of Secs. VC and VII A 2, the previous and the present model are compared in this Appendix. Figure 7 shows the density profiles at the stationary state obtained by the respective models for cases C2 and C4 with $K = 1.0 \times 10^{-4}$, see Fig. 1. As seen from the figure, the densities at the flat parts do not agree between the models. This is in marked contrast to the agreement of the stability criterion discussed in Sec. VB. The discrepancy in quantity comes from the fact that the previous isothermal model was thermodynamically designed for the system in contact

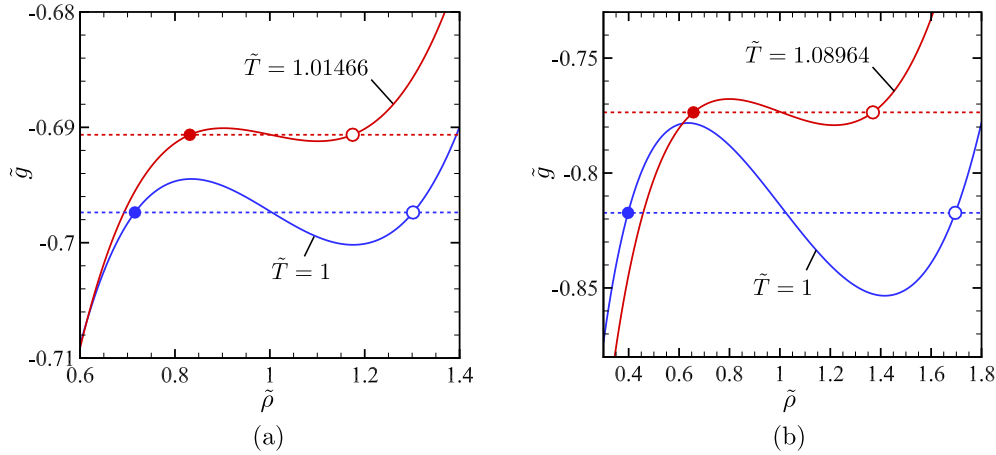


FIG. 8. The equiarea rule applied to \tilde{g} for the previous and the present model. (a) Case C2 and (b) case C4. The horizontal coordinate of the open circle and that of the closed circle indicate ρ_A/ρ_0 and ρ_B/ρ_0 , respectively.

with the thermal bath through its collision term. The physical system in the present paper is thermodynamically isolated and thus the temperature is no longer constant. The temperature change is rather small but the two phase densities are sensitive to the change of temperature, as is explained below.

By using the method in Sec. VII B, the temperature after the phase transition in the present model is computed as $\tilde{T} = 1.01466$ for case C2 and $\tilde{T} = 1.08964$ for case C4. Since the difference of temperature is small (at least for case C2), one may wonder why such a distinct difference occurs in density. The reason is as follows. In the previous model, the densities of two phases after the phase transition have been predicted by applying the equiarea rule to $\Phi(\tilde{\rho})$ of Ref. [15]. In viewing its functional form, it is essentially identical to the specific Gibbs energy g in the present model at the stationary state, see (22). Remember that the VDF is the Maxwellian with the

uniform temperature in the stationary state. Introducing the dimensionless version of g after getting rid of the constant terms with respect to ρ by

$$\tilde{g}(\tilde{\rho}, \tilde{T}) = \tilde{\Phi}_S + \frac{1}{2} \tilde{T} \ln \tilde{\rho},$$

the $\Phi(\tilde{\rho})$ in Ref. [15] is equivalent to $\tilde{g}(\tilde{\rho}, 1) + 1/2$. Therefore, the densities of two phases after the phase transition can be predicted by applying the equiarea rule to $\tilde{g}(\tilde{\rho}, 1)$ for the previous model and $\tilde{g}(\tilde{\rho}, \tilde{T})$ for the present model, where \tilde{T} is the uniform temperature in the stationary state. As shown in Fig. 8, the difference of temperature affects the density values determined by the equiarea rule. Case C2 with $\tilde{T} = 1$ gives $\rho_A/\rho_0 = 1.30198$ and $\rho_B/\rho_0 = 0.71555$, while that with $\tilde{T} = 1.01466$ gives $\rho_A/\rho_0 = 1.17466$ and $\rho_B/\rho_0 = 0.83128$. Case C4 with $\tilde{T} = 1$ gives $\rho_A/\rho_0 = 1.69571$ and $\rho_B/\rho_0 = 0.39755$, while that with $\tilde{T} = 1.08964$ gives $\rho_A/\rho_0 = 1.36906$ and $\rho_B/\rho_0 = 0.65703$.

- [1] J. O. Hirschfelder, C. F. Curtiss, and R. B. Bird, *Molecular Theory of Gases and Liquids* (John Wiley & Sons, New York, 1964).
- [2] C. Cercignani, *The Boltzmann Equation and Its Applications* (Springer-Verlag, New York, 1988).
- [3] Y. Sone, *Molecular Gas Dynamics* (Birkhäuser, Boston, 2007); Supplementary Notes and Errata is available from Kyoto University Research Information Repository, <http://hdl.handle.net/2433/66098>.
- [4] D. Enskog, Kinetische theorie der wärmeleitung, reibung and selbstdiffusion in gewissen verdichteten gasen und flüssigkeiten, K. Sven. Vetenskapsakad. Handl. **63**, 3 (1922); English translation is available from Brush, S. G.: *Kinetic Theory*, Vol. 3 (Pergamon, Oxford, 1972), p. 226.
- [5] S. Chapman and T. Cowling, *The Mathematical Theory of Non-uniform Gases*, 3rd ed. (Cambridge University Press, Cambridge, 1970).
- [6] M. Grmela, Kinetic equation approach to phase transitions, *J. Stat. Phys.* **3**, 347 (1971).
- [7] A. Frezzotti, L. Gibelli, and S. Lorenzani, Mean field kinetic theory description of evaporation of a fluid into vacuum, *Phys. Fluids* **17**, 012102 (2005).
- [8] K. Kobayashi, K. Ohashi, and M. Watanabe, Numerical analysis of vapor-liquid two-phase system based on the Enskog-Vlasov equation, *AIP Conf. Proc.* **1501**, 1145 (2012).
- [9] A. Frezzotti and P. Barbante, Kinetic theory aspects of non-equilibrium liquid-vapor flows, *Mech. Eng. Rev.* **4**, 16-00540 (2017).
- [10] A. Frezzotti, P. Barbante, and L. Gibelli, Direct simulation Monte Carlo applications to liquid-vapor flows, *Phys. Fluids* **31**, 062103 (2019).
- [11] S. Busuioc, L. Gibelli, D. A. Lockerby, and J. E. Sprittles, Velocity distribution function of spontaneously evaporating atoms, *Phys. Rev. Fluids* **5**, 103401 (2020).
- [12] S. Busuioc and L. Gibelli, Mean-field kinetic theory approach to Langmuir evaporation of polyatomic liquids, *Phys. Fluids* **32**, 093314 (2020).
- [13] V. Giovangigli, Kinetic derivation of diffuse-interface fluid models, *Phys. Rev. E* **102**, 012110 (2020).

- [14] S. Takata and T. Noguchi, A simple kinetic model for the phase transition of the van der Waals fluid, *J. Stat. Phys.* **172**, 880 (2018).
- [15] S. Takata, T. Matsumoto, A. Hirahara, and M. Hattori, Kinetic theory for a simple modeling of a phase transition: Dynamics out of local equilibrium, *Phys. Rev. E* **98**, 052123 (2018).
- [16] H. van Beijeren and M. H. Ernst, The modified Enskog equation, *Physica* **68**, 437 (1973).
- [17] P. Resibois, H-theorem for the (modified) nonlinear Enskog equation, *J. Stat. Phys.* **19**, 593 (1978).
- [18] P. Maynar, M. I. García de Soria, and J. J. Brey, The Enskog equation for confined elastic hard spheres, *J. Stat. Phys.* **170**, 999 (2018).
- [19] E. S. Benilov and M. S. Benilov, Energy conservation and H theorem for the Enskog–Vlasov equation, *Phys. Rev. E* **97**, 062115 (2018).
- [20] P. L. Bhatnagar, E. P. Gross, and M. Krook, A model for collision processes in gases. I. Small amplitude processes in charged and neutral one-component systems, *Phys. Rev.* **94**, 511 (1954).
- [21] J. S. Rowlinson and B. Widom, *Molecular Theory of Capillarity* (Dover, New York, 1982).
- [22] L. M. Pismen and Y. Pomeau, Disjoining potential and spreading of thin liquid layers in the diffuse-interface model coupled to hydrodynamics, *Phys. Rev. E* **62**, 2480 (2000).
- [23] J. M. Smith, H. C. Van Ness, and M. M. Abbott, *Introduction to Chemical Engineering Thermodynamics*, 5th ed. (McGraw-Hill, New York, 1996), Sec. 13.4.
- [24] The first identity is shown to hold as follows:

$$\begin{aligned} & m \int_D \rho(\mathbf{X}) \frac{\partial \Phi_L}{\partial X_j} d\mathbf{X} \\ &= \int_D \rho(\mathbf{X}) \int_{\mathbb{R}^3} \Psi(|\mathbf{r}|) \frac{\partial}{\partial X_j} \{\rho(\mathbf{X} + \mathbf{r}) - \rho(\mathbf{X})\} d\mathbf{r} d\mathbf{X} \\ &= \int_D \rho(\mathbf{X}) \int_{\mathbb{R}^3} \Psi(|\mathbf{Y} - \mathbf{X}|) \frac{\partial}{\partial Y_j} \rho(\mathbf{Y}) d\mathbf{Y} d\mathbf{X} \\ &= - \int_D \rho(\mathbf{X}) \int_{\mathbb{R}^3} \rho(\mathbf{Y}) \frac{\partial}{\partial Y_j} \Psi(|\mathbf{Y} - \mathbf{X}|) d\mathbf{Y} d\mathbf{X} \\ &= \frac{1}{2} \int_D \rho(\mathbf{X}) \int_{\mathbb{R}^3} \rho(\mathbf{Y}) \left\{ \frac{\partial \Psi}{\partial X_j} - \frac{\partial \Psi}{\partial Y_j} \right\} d\mathbf{Y} d\mathbf{X}, \end{aligned}$$

where the dependence on t is suppressed for the brevity of notation. In the above transformation, besides the integration by parts, it has been used that $\rho(\mathbf{X})$ is periodic in \mathbf{X} and that Ψ decays sufficiently fast with respect to its argument. Since the last integrand is periodic in \mathbf{X} , the infinite sum of the last double integral leads to

$$\frac{1}{2} \int_{\mathbb{R}^3} \rho(\mathbf{X}) \int_{\mathbb{R}^3} \rho(\mathbf{Y}) \left\{ \frac{\partial}{\partial X_j} - \frac{\partial}{\partial Y_j} \right\} \Psi d\mathbf{Y} d\mathbf{X},$$

which is identical to zero. Hence,

$$\int_D \rho(\mathbf{X}) \frac{\partial \Phi_L}{\partial X_j} d\mathbf{X} = 0,$$

holds. As to the second identity, by the integration by parts and the use of the mass conservation, it is enough to show that

$$\int_D \Phi_L \frac{\partial \rho}{\partial t} d\mathbf{X} = \frac{1}{2} \frac{\partial}{\partial t} \int_D \Phi_L \rho d\mathbf{X}.$$

Since the integrands in the above are periodic, one can prove the above by showing the identity below, which is easier to handle:

$$\begin{aligned} & m \int_{\mathbb{R}^3} \left\{ \Phi_L \frac{\partial \rho}{\partial t} - \frac{1}{2} \frac{\partial}{\partial t} (\Phi_L \rho) \right\} d\mathbf{X} \\ &= \int_{\mathbb{R}^3} \int_{\mathbb{R}^3} \left[\Psi(r) \{ \rho(t, \mathbf{Y}) - \rho(t, \mathbf{X}) \} \frac{\partial}{\partial t} \rho(t, \mathbf{X}) \right. \\ &\quad \left. - \frac{1}{2} \Psi(r) \frac{\partial}{\partial t} [\rho(t, \mathbf{X}) \{ \rho(t, \mathbf{Y}) - \rho(t, \mathbf{X}) \}] \right] d\mathbf{Y} d\mathbf{X} \\ &= \int_{\mathbb{R}^3} \int_{\mathbb{R}^3} \left[\Psi(r) \{ \rho(t, \mathbf{Y}) - \rho(t, \mathbf{X}) \} \frac{\partial}{\partial t} \rho(t, \mathbf{X}) \right. \\ &\quad \left. - \frac{1}{2} \Psi(r) \{ \rho(t, \mathbf{Y}) - \rho(t, \mathbf{X}) \} \frac{\partial}{\partial t} \rho(t, \mathbf{X}) \right. \\ &\quad \left. - \frac{1}{2} \Psi(r) \rho(t, \mathbf{X}) \frac{\partial}{\partial t} \{ \rho(t, \mathbf{Y}) - \rho(t, \mathbf{X}) \} \right] d\mathbf{Y} d\mathbf{X} \\ &= \int_{\mathbb{R}^3} \int_{\mathbb{R}^3} \left[\Psi(r) \rho(t, \mathbf{Y}) \frac{\partial}{\partial t} \rho(t, \mathbf{X}) \right. \\ &\quad \left. - \frac{1}{2} \Psi(r) \rho(t, \mathbf{Y}) \frac{\partial}{\partial t} \rho(t, \mathbf{X}) \right. \\ &\quad \left. - \frac{1}{2} \Psi(r) \rho(t, \mathbf{X}) \frac{\partial}{\partial t} \rho(t, \mathbf{Y}) \right] d\mathbf{Y} d\mathbf{X} = 0, \end{aligned}$$

where $r = |\mathbf{Y} - \mathbf{X}|$. Thanks to the periodicity of ρ , the proof of the identities in the case of the approximation $\Phi_L = -\kappa \partial^2 \rho / \partial X_i^2$ is straightforward and is omitted here.

- [25] The identity is shown to hold as follows:

$$\begin{aligned} & \int_{\mathbb{R}^3} \{ \rho \Phi_L [\delta \rho] - \Phi_L [\rho] \delta \rho \} d\mathbf{X} \\ &= \int_{\mathbb{R}^3} \rho(\mathbf{X}) \int_{\mathbb{R}^3} \Psi(r) \{ \delta \rho(\mathbf{Y}) - \delta \rho(\mathbf{X}) \} d\mathbf{Y} d\mathbf{X} \\ &\quad - \int_{\mathbb{R}^3} \delta \rho(\mathbf{X}) \int_{\mathbb{R}^3} \Psi(r) \{ \rho(\mathbf{Y}) - \rho(\mathbf{X}) \} d\mathbf{Y} d\mathbf{X} \\ &= \int_{\mathbb{R}^3} \rho(\mathbf{X}) \int_{\mathbb{R}^3} \Psi(r) \delta \rho(\mathbf{Y}) d\mathbf{Y} d\mathbf{X} \\ &\quad - \int_{\mathbb{R}^3} \delta \rho(\mathbf{X}) \int_{\mathbb{R}^3} \Psi(r) \rho(\mathbf{Y}) d\mathbf{Y} d\mathbf{X} = 0, \end{aligned}$$

where $r = |\mathbf{X} - \mathbf{Y}|$. Then, because $\int_{\mathbb{R}^3} \Psi(r) \rho(\mathbf{Y}) d\mathbf{Y}$ as well as ρ and $\delta \rho$ is periodic in \mathbf{X} , the above identity is reduced to $\int_D \{ \rho \Phi_L [\delta \rho] - \Phi_L [\rho] \delta \rho \} d\mathbf{X} = 0$. In the case $\Phi_L = -\kappa \partial^2 \rho / \partial X_i^2$, the desired identity is simply obtained by the repeated integration by parts.

- [26] E. S. Benilov and M. S. Benilov, Semiphenomenological model for gas-liquid phase transitions, *Phys. Rev. E* **93**, 032148 (2016).

- [27] Since the bulk modulus k_T is defined by

$$k_T = \rho \left(\frac{\partial p}{\partial \rho} \right)_T = \rho^2 RT \left(\frac{1}{\rho} + \frac{\Phi_\rho}{RT} \right),$$

the stable condition (25a) is identical to the condition $k_T > 0$. In the case the density increase induces the pressure increase, which in turn induces the mass flow from the density-increased spot, suppressing the density increase. Hence, the disturbance does not develop.

- [28] E. S. Benilov and M. S. Benilov, The Enskog–Vlasov equation: A kinetic model describing gas, liquid, and solid, *J. Stat. Mech.* (2019) 103205.

- [29] E. Fermi, *Thermodynamics* (Dover, New York, 1956).
 [30] Van P. Carey, *Liquid–Vapor Phase-change Phenomena* (Taylor & Francis, Bristol, 1992).
 [31] Under the approximation $\Phi_L = -\kappa \partial^2 \rho / \partial X_i^2$, (30) is eventually reduced to

$$\frac{\partial}{\partial X_j} \left(p \delta_{ij} - \kappa \left\{ \rho \frac{\partial^2 \rho}{\partial X_k^2} + \frac{1}{2} \left(\frac{\partial \rho}{\partial X_k} \right)^2 \right\} \delta_{ij} + \kappa \frac{\partial \rho}{\partial X_i} \frac{\partial \rho}{\partial X_j} \right) = 0.$$

On the plateau, the gradients of density all vanish and only the first term in parentheses remains.

- [32] By changing the scale of spatial coordinates as $Y_i = X_i / \sqrt{\kappa}$, the contribution is rewritten as

$$\int_D \rho \Phi_L dX = -\kappa^{3/2} \int_{D_Y} \rho \frac{\partial^2 \rho}{\partial Y_i^2} dY,$$

where D_Y is the counterpart of D in the Y -space. Since the integrand and its support are of the order unity, the contribution tends to vanish as $\kappa \rightarrow 0$.

- [33] V. Giovangigli, *Multicomponent Flow Modeling* (Birkhäuser, Boston, 1999).
 [34] E. Nagnibeda and E. Kustova, *Non-Equilibrium Reacting Gas Flows* (Springer–Verlag, Berlin, 2009).
 [35] See Supplemental Material at <https://link.aps.org/supplemental/10.1103/PhysRevE.103.062110> for additional figures on the influence of K and k .
 [36] R. Soto, *Kinetic Theory and Transport Phenomena* (Oxford University Press, Clarendon, 2017).
 [37] Unfortunately, in the case of the approximated form $\Phi_L = -\kappa \partial^2 \rho / \partial X_i^2$, the same transformation does not apply because the approximation violates a symmetric property in part in the original form of Φ_L .
 [38] This includes the diffuse reflection, the Maxwell, and the Cercignani–Lampis condition as specific examples. See, e.g., Refs. [2,3].
 [39] J. S. Darrozes and J. P. Guiraud, Généralisation formelle du théorème H en présence de parois. Applications, C. R. Acad. Sci. Paris A **262**, 1368 (1966).